ABSTRACT

Systems modeled using differential equations often include a continuous disturbance. In reality, disturbances usually occur at discrete times. To what extent do the predictions of these continuous models still hold when the disturbance is instead applied at discrete time intervals? In this thesis, we investigate the FitzHugh-Nagumo system of differential equations with flow-kick disturbances. We use numerical continuation in MatContM to find bifurcations and study solution behavior. In particular, we investigate bifurcations that are bounded away from the continuous system in parameter space. Using numerical simulation, we observe and describe behavior in regions of parameter space where MatContM continuation fails. We also use symbolic dynamics to observe period adding bifurcations in a novel class of dynamical systems.

Bifurcation Analysis of the Flow-Kick FitzHugh-Nagumo System of Differential Equations

Jayson Ruml

Advisor
Alanna Hoyer-Leitzel

A thesis submitted to the Department of Mathematics and Statistics in partial fulfillment of the requirements for the degree of Bachelor of Arts with Honors

Department of Mathematics and Statistics
Mount Holyoke College
South Hadley, MA 01075
May 2026

ACKNOWLEDGEMENTS

This thesis would not have even been conceptualized without the support and encouragement of my advisor, Alanna Hoyer-Leitzel. Taking Intro to Proofs with you led me to become a math major, and your encouragement to pursue research has absolutely changed my academic career. Thank you for putting up with my truly horrendous first drafts and absolute lack of tech ability, and for teaching me how to organize things in folders on my desktop. Thank you also for allowing me to be a human being throughout this process. I'm so grateful to have had you as a professor.

I would also like to thank my major advisor and committee member Lidia Mrad. It was a pleasure to work with you as a TA and I deeply appreciate the conversations we have had over the course of my time in the department. I am also grateful to Spencer Smith for his willingness to serve on my committee.

I would like to extend my deepest love and gratitude to my friends and family who have supported me throughout the research process. First, thank you to Gita, who made me promise I would drop this thesis if it meant that I couldn't hang out with her. I feel lucky to have you in my life and very lucky that I was able to do both. Thank you to Madigan for your thesis solidarity - I can't wait to get sushi with you when we're done. Thank you to Valentina, Luca, Charlotte, Morgan, and Finn for sprinting across the Smith College campus and getting into a locked basement to listen to me talk about my work. I don't know what I did to deserve you all, but I would not have gotten through college without you. Thank you to my sister, Geneva, for believing in me and thinking I'm cool. Finally, thank you to my mama for sitting with me at Crackskull's while I worked, visiting me at my summer research, and making sure I always know that I'm loved.

I am grateful to my fellow 2025 student summer researchers for their warmth and community. Without them, staying on campus over the summer would have been much lonelier.

I would also like to acknowledge the use of ChatGPT for preliminary coding work. No AI was used in the writing of this thesis.

Contents

List of Figures

List of Tables

Chapter 1

Introduction

In a differential equation $\dot{x} = f(x, \mu)$, a bifurcation occurs when a small, continuous change in the value of one or more parameters leads to a sudden qualitative change in solution behavior. A well-known example is a simple population model with a constant harvesting parameter—if the harvesting parameter is low, populations will asymptotically approach either the carrying capacity or extinction, depending on the initial population. However, once the harvesting parameter reaches a certain value, it will become impossible for population growth to outpace harvesting, and there will only be one possible solution behavior: extinction. This qualitative change in solution behavior as the parameter value shifts is an example of a bifurcation.

There are two notable types of solution behaviors that can be created, destroyed, or altered at a bifurcation. A fixed point is a solution that remains constant for all time, ie. $f(x^*, \mu) = 0$ for all t. A periodic solution returns to the same value at regular time intervals, repeating its trajectory every T time units. We will use numerical simulation to find parameter values at which these types of behavior occur, and use this information to locate bifurcations in parameter space.

A map is a different way of modeling the evolution of a system, where time is taken in discrete steps rather than flowing continuously. For each iteration, the map function takes as its input the previous step and outputs the current step, ie. $x_{n+1} = f(x_n, \mu)$ where f is the map function (13). Like ordinary differential equations, maps can undergo bifurcations as parameter values are shifted. In this thesis, we will study a type of map called a flow-kick map.

A flow-kick map is a specific type of map that allows us to model a flow governed by a differential equation interrupted by discrete disturbances. The *flow* component of the map is completely determined by the underlying ordinary differential equation, with the flow at time t given a certain starting point defined as the solution to the underlying system at time t with that initial condition. The other component of the flow-kick map, the *kick*, represents a discrete, instantaneous disturbance in the flow. For each iteration of the flow-kick map, we calculate the flow as governed by the underlying system for time $t = \tau$, and then apply a disturbance k. The next iteration of the map begins at this new point in state space. More information about the flow-kick concept is available in (11; 12; 15). Notably, for small enough τ, some types of bifurcations can continue from the underlying system to the flow-kick map (12).

Motivation to study flow-kick maps comes from ecological applications such as natural resource management (9; 11; 15). While ecosystem dynamics can be modeled by ordinary differential equations, inaccuracies can arise when occasional, discrete disturbances such as rain in a desert are represented as continuous parameters. In these situations, flow-kick maps may provide more accurate models (15). There are often large, qualitative differences in the predictions of ordinary differential equations and flow-kick maps, even when the average rate of disturbance is the same (9). Aside from the potential ecological applications, the differences in

behavior between ordinary differential equations and flow-kick maps are intriguing. Here, we will focus on a mathematical study of a specific flow-kick system for its own sake rather than on solving an applied problem.

We will consider the FitzHugh-Nagumo model, a two-dimensional system of differential equations used to model systems that exhibit excursions, such as spiking neurons. The continuous FitzHugh-Nagumo system is defined as:

$$\dot{x} = x(1-x)(x-2) - y$$
$$\dot{y} = 0.1(x - 0.2) - r$$

where r is a parameter. The continuous system undergoes two Hopf bifurcations as r is varied, with stable fixed points existing above and below the Hopf bifurcation points and a stable periodic orbit between them.

Previously, the FitzHugh-Nagumo system has been studied with discrete stochastic disturbances (10). We will examine the behavior of the system with discrete, deterministic disturbances.

In Chapter 2, we provide the necessary background information and definitions for our research. We begin by defining critical types of solution behavior that we observe in our system. We define the flow-kick map, and give the flow-kick map governed by the continuous FitzHugh-Nagumo system. We also examine the behavior of the underlying continuous system, defining and locating the Hopf bifurcation points.

In Chapter 3, we use numerical methods to study solution behavior of the flow-kick FitzHugh-Nagumo system with varied parameter values. In Section 3.1, we use numerical simulation to find regions of existence of stable structures (fixed points and periodic solutions) in τk-parameter space. We find a region of periodic

and quasiperiodic solutions with three distinct boundary curves. One of these curves is bounded away from the $\tau = 0$ axis, meaning that it is extremely unlikely that it represents a bifurcation that continues from the underlying system. In Section 3.2, we use similar numerical techniques to observe the period of each solution in the periodic region. We use this information to determine the type of bifurcation that occurs as we cross the boundary from the fixed point region to the periodic region.

We build upon this work in Chapter 4 by using numerical continuation to find and continue bifurcation curves in parameter space. The bifurcation curves that we find align with the boundaries of the periodic region found in Chapter 3. Section 4.1 provides the theoretical underpinnings of the numerical continuation technique, which relies on the Implicit Function Theorem. We also discuss the mechanism by which MatContM finds and continues bifurcation curves. In Section 4.2, we compare our continuation results with our results from Chapter 3. We find that the top and bottom-left boundaries correspond to two Neimark-Sacker bifurcation curves. We also observe a period-doubling bifurcation curve branching off of each Neimark-Sacker curve. Notably, numerical continuation fails near the bottom-right boundary, which is bounded away from the $\tau = 0$ axis.

In Chapter 5, we focus on the bottom-right boundary of the periodic region, where previous methods were not able to identify the bifurcation type. In Section 5.1, we create bifurcation diagrams in each of our parameters, k and τ, near the boundary. As τ is varied, we observe a period incrementing structure, where we see intervals of solutions with a constant period n, then a region of variable, higher periods, and then another interval of solutions with period $n + 1$. As k is varied, we briefly observe a similar incrementing structure, then a long interval of period 2 solutions, then another higher-period region before transitioning back to

a 3-periodic interval and then to a fixed point at a new location in state space. We compare these results to existing research on the period adding and period incrementing bifurcation structures (7).

In Section 5.2, we introduce symbolic dynamics as a technique for comparing our system's behavior to the period adding and period incrementing bifurcation structures. We begin by providing relevant definitions and background information, and establish how we will define symbolic sequences for this system. We present the results of our symbolic dynamics investigation and compare them with the definitions presented in the symbolic dynamics literature (7). The full symbolic dynamics data tables are in Appendices A and B.

Chapter 2

Background

In this chapter, we introduce the necessary background for our work. We provide definitions and necessary conditions for bifurcations of both continuous differential equations and discrete maps. We define the flow-kick FitzHugh-Nagumo system, and analyze the behavior of the underlying continuous system.

2.1 Equilibria and Limit Cycles of Continuous Differential Equations

Let $\dot{x} \in \mathbb{R}^2$, and let $f : \mathbb{R}^2 \times \mathbb{R} \to \mathbb{R}^2$ be a smooth function. Consider the system $\dot{x} = f(x, \mu)$ where μ is a parameter.

Definition 2.1.1 (Flow)**.** Given a differential equation $\dot{x} = f(x, \mu)$, denote the flow of the equation as ϕ_t, so that the solutions can be written $x(t) = \phi_t(x_0)$. This means that the solution $x(t)$ is equal to the flow for time t starting at the initial condition x_0 (13).

We will begin by defining two special types of solutions to the system.

Definition 2.1.2 (Fixed point/equilibrium solution)**.** A *fixed point* or *equilibrium solution* to the equation $\dot{x} = f(x, \mu)$ is a constant function such that $f(x, \mu) = 0$. In other words, the rate of change of the solution is always zero; it has the same value for all time (4).

In order to evaluate the stability of a fixed point, we will need to introduce the Jacobian matrix:

Definition 2.1.3 (Jacobian matrix)**.** The *Jacobian matrix* J of a system $\dot{x} = f(x, \mu)$ is the matrix

$$J = \begin{bmatrix} \frac{\partial f_1}{\partial x_1} & \frac{\partial f_1}{\partial x_2} \\ \frac{\partial f_2}{\partial x_1} & \frac{\partial f_2}{\partial x_2} \end{bmatrix}$$

(13).

Definition 2.1.4 (Stable equilibrium solution)**.** Let x^* be an equilibrium solution to the equation $\dot{x} = f(x, \mu)$. Then x^* is called *stable* when for all $\epsilon > 0$ there exists $\delta > 0$ such that if $|x(0) - x^*| < \delta$, then $|x(t) - x^*| < \epsilon$ for all $t > 0$. If $\lim_{t\to\infty} x(t) = x^*$, then x^* is *asymptotically stable*. In other words, all solutions starting sufficiently close to the stable equilibrium point asymptotically approach the equilibrium solution.

The stability of a fixed point can be determined by finding the eigenvalues of the Jacobian matrix at the fixed point. If both eigenvalues have $Re(\lambda) < 0$, the fixed point is stable (13).

An equilibrium solution is called *unstable* when it is not stable. If at least one eigenvalue λ of the Jacobian has $Re(\lambda) > 0$, the fixed point is unstable (13). If $\lim_{t\to-\infty} x(t) = x^*$, then x^* is *repelling*.

Definition 2.1.5 (Saddle point)**.** An equilibrium solution is called a *saddle point* when it has one real eigenvalue greater than zero and one real eigenvalue less than zero. At a saddle point, the phase space of the linearized system is divided into a stable subspace and an unstable subspace, with solutions in the stable subspace moving towards the saddle point and solutions in the unstable subspace repelled away from it (8).

Unstable, repelling, and saddle solutions are not detectable using numerical simulation since solutions with arbitrarily close initial conditions are repelled away over time.

Definition 2.1.6 (Limit cycle/periodic solution)**.** A *limit cycle* or *periodic solution* to the equation $\dot{x} = f(x, \mu)$ is a solution $x(t)$ such that for some $T > 0$, $x(t+T) = x(t)$ for all t. This means that $x(t)$ returns to the same value at regular time intervals, repeating its trajectory exactly every T time units (8).

Definition 2.1.7 (Bifurcation)**.** A *bifurcation* occurs when a small, continuous change in the value of one or more parameters of a dynamical system causes a sudden, qualitative change in solution behavior.

There are several types of bifurcations, each with their own characteristics and necessary conditions. Bifurcations may involve, for example, the creation or destruction of fixed points or periodic solutions, or a change in the stability of a fixed point. We begin by defining the most common type of bifurcation for 1-dimensional systems.

Definition 2.1.8 (Saddle-node bifurcation)**.** A *saddle-node bifurcation* is characterized by one stable and one unstable equilibrium point colliding and annihilating each other as a parameter is varied (13). The value of the parameter μ^* at the

moment the fixed points collide is called the saddle-node bifurcation point. This type of bifurcation occurs when the Jacobian matrix at the fixed point (x^*, μ^*) has a zero eigenvalue.

In two-dimensional systems, more complex types of bifurcations are possible.

Definition 2.1.9 (Supercritical Hopf bifurcation)**.** A *supercritical Hopf bifurcation* (see Figure 2.1) is characterized by a stable equilibrium point losing stability (becoming an unstable equilibrium point) and the birth of a stable limit cycle around the new unstable equilibrium point. Solutions with initial conditions outside the new limit cycle continue to asymptotically approach the limit cycle, but solutions with initial conditions inside the limit cycle are repelled away from the unstable fixed point and asymptotically approach the limit cycle.

Hopf bifurcations occur when the real part of both eigenvalues of the Jacobian matrix simultaneously change sign (13).

2.2 Fixed Points and Limits Cycles of Maps

In the previous section, we defined structures for differential equations in continuous time. Now we'll define the same phenomena for maps, which take time in discrete steps.

Let $\dot{x} \in \mathbb{R}^2$, and let $f : \mathbb{R}^2 \times \mathbb{R} \to \mathbb{R}^2$ be a smooth function. We'll consider the iterated map $x_{n+1} = f(x_n, \mu)$ where μ is a parameter.

Definition 2.2.1 (Orbit)**.** An *orbit* of a differential equation is the set of points in state space covered by the evolution of the equation beginning at a particular initial condition (13).

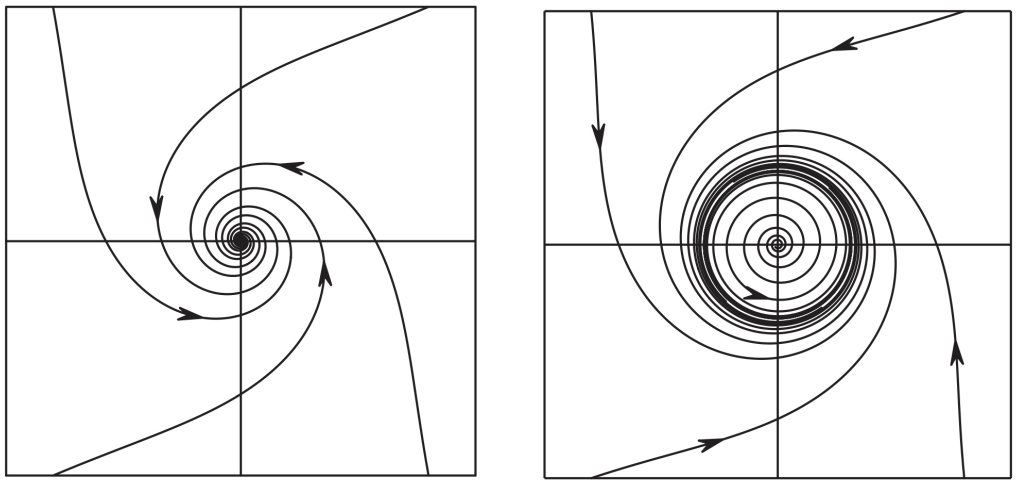

Figure 2.1: Supercritical Hopf bifurcation (Image from (8)). At the moment of bifurcation, the equilibrium point at the origin switches from stable to unstable, and a stable limit cycle is born to which solutions close to the equilibrium point are now attracted.

Definition 2.2.2 (Fixed point of maps)**.** For a map $x_{n+1} = f(x_n, \mu)$, a point x^* is a *fixed point* if $f(x^*, \mu) = x^*$ (13). Informally, at each iteration of the map, the input and output are the same, meaning that the trajectory of the map remains at x_0 for all time.

The concept of stability for fixed points of maps is similar to continuous differential equations, but stability is calculated differently.

Definition 2.2.3 (Stable fixed point of a map)**.** A fixed point x^* of a map $x_{n+1} = f(x_n, \mu)$ is *stable* if solutions with initial conditions near the fixed point are attracted towards it, ie. small disturbances are damped over time. Similarly to equilibrium solutions of continuous differential equations, if $\lim_{n\to\infty} x_n = x^*$, then x^* is *asymptotically stable*.

The stability of a fixed point of a map can be determined by calculating the eigenvalues λ_1, λ_2 of the Jacobian of the map at the fixed point. If $|\lambda_1| < 1$ and

$|\lambda_2|< 1$, then the fixed point is stable (13).

A fixed point of a map is *unstable* if it is not stable. If at least one of the eigenvalues of the Jacobian matrix at a fixed point has magnitude greater than 1, then the fixed point is unstable. If $\lim_{n\to-\infty} x_n = x^*$, then x^* is *repelling*.

Definition 2.2.4 (Saddle point for a map)**.** A fixed point of a map is called a *saddle point* when $|\lambda_1|< 1$ and $|\lambda_2|> 1$ (1). At a saddle point, the phase space of the linearized system is divided into a stable subspace and an unstable subspace, with solutions in the stable subspace moving towards the saddle point and solutions in the unstable subspace repelled away from it (8).

As is the case for ordinary differential equations, unstable fixed points of maps are not detectable using numerical simulation.

Definition 2.2.5 (Periodic orbit for a map)**.** For a map defined by a function $f(x, \mu)$, a *periodic orbit with period n* is a point x^* such that $f^n(x^*, \mu) = x^*$ for some $n > 1$(8). In other words, the orbit takes the same value every n iterations of the map.

Definition 2.2.6 (Bifurcation of a map)**.** A map defined by a function $f(x, \mu)$ undergoes a *bifurcation* when a small, continuous change in the value of the parameter results in a sudden, qualitative change in solution behavior.

We will come across several types of map bifurcations in our investigation. One that will be particularly important is the Neimark-Sacker bifurcation, which is analogous to the Hopf bifurcation in the continuous system.

Definition 2.2.7 (Supercritical Neimark-Sacker bifurcation)**.** Like the supercritical Hopf bifurcation, the *supercritical Neimark-Sacker bifurcation* is characterized

by a stable fixed point losing stability and the birth of a stable limit cycle around the new unstable fixed point (14).

The conditions for the existence of a Neimark-Sacker bifurcation are also similar to the Hopf bifurcation, since both involve a fixed point crossing the boundary from stable to unstable and the creation of a stable limit cycle. For a Neimark-Sacker bifurcation, both eigenvalues of the Jacobian matrix must cross the unit circle, ie. have modulus 1 and a nonzero derivative. The eigenvalues also must not be a 1st, 2nd, 3rd, or 4th root of unity ($\lambda^n \neq 1$ for $n = 1, 2, 3, 4$). This is because other types of bifurcations occur at these roots of unity: the 1st root of unity gives a saddle node bifurcation, the 2nd gives a period doubling bifurcation, and the 3rd and 4th respectively represent the transition from a fixed point to a 3-cycle or a 4-cycle.

Definition 2.2.8 (Period-doubling bifurcation)**.** The period-doubling bifurcation is characterized by a stable n-periodic orbit becoming unstable and the creation of a new stable $2n$-periodic orbit.

In order for a period-doubling bifurcation to occur, there must exist one eigenvalue λ_i of the Jacobian matrix of $f^n(x, \mu)$ such that $\lambda_i = 1$ (14).

2.3 Flow-Kick Maps

A flow-kick map is a type of hybrid system or impulsive differential equation that models a flow governed by a continuous differential equation interrupted by discrete disturbances, which can be more realistic for some modeling applications (9; 11; 15). The flow component is completely determined by the underlying ordinary differential equation, and the kick represents a discrete, instantaneous disturbance in state space.

Definition 2.3.1 (Impulsive differential equation)**.** Let $f(t, x(t))$ be a smooth function. Let $k = 1, 2...m$. An impulsive differential equation can be defined as follows:

$$\dot{x}(t) = f(t, x(t)), t \neq t_k$$
$$\Delta x(t_k) = I_k(x(t_k^{-m})), t = t_k$$

where I_k is an impulse function representing the jump of the state at each t_k (2).

Definition 2.3.2 (Flow-kick map)**.** Let $\phi_\tau(x)$ represent the flow for the differential equation $\dot{x} = f(x, \mu)$ starting at the point x at time $t = 0$ until time $t = \tau$. Let k represent the magnitude of a discrete disturbance (kick). Then we define a flow-kick map as

$$G_{\tau,k}(x) = \phi_\tau(x) + k$$

The map is iterated to give a trajectory where $x_i = G_{\tau,k}(x_{i-1})$ (15).

The flow-kick map has two parameters, τ and k, both of which may be varied in order to detect bifurcations.

2.4 FitzHugh-Nagumo System

This thesis will study the FitzHugh-Nagumo system of differential equations, defined as:

$$\begin{aligned} \dot{x} &= x(1-x)(x-2) - y \\ \dot{y} &= 0.1(x - 0.2) - r \end{aligned} \tag{2.1}$$

where $\dot{x}$ denotes the rate of change of x, $\dot{y}$ denotes the rate of change of y, and r is a parameter whose value we will vary.

As r is varied, the system undergoes two supercritical Hopf bifurcations, one in forward time and one in backwards time. At the first Hopf bifurcation point, the system's stable equilibrium point loses stability and a stable limit cycle is created. At the second, backwards time bifurcation, the limit cycle disappears and the fixed point regains stability.

Since it is nontrivial to find the Hopf bifurcations using the Jacobian matrix, we employ a geometric technique based on nullclines to calculate the values of r where the bifurcations occur. The continuous FitzHugh-Nagumo system has two nullclines: a cubic nullcline given by $y = -x(x-1)(x-2)$, whose location in the xy-plane is fixed, and a vertical line nullcline $x = 10r + 0.2$. The Hopf bifurcations occur when the intersection of the nullclines takes place at either the local minimum or the local maximum of the cubic nullcline (see Figure 2.2). We find that these intersections occur when $r = 0.08 + \frac{0.1}{\sqrt{3}}$ and $r = 0.08 - \frac{0.1}{\sqrt{3}}$. For $0.08 - \frac{0.1}{\sqrt{3}} < r < 0.08 + \frac{0.1}{\sqrt{3}}$ (between the bifurcation points), a stable limit cycle exists. For values of r less than $0.08 - \frac{0.1}{\sqrt{3}}$ or greater than $0.08 + \frac{0.1}{\sqrt{3}}$, a stable fixed point exists.

The focus of this thesis will be on the flow-kick map with flow governed by the FitzHugh-Nagumo system with $r = 0$ as both parameters τ, k are varied. The flow-kick map governed by the FitzHugh-Nagumo system can be represented as

$$G_{\tau,k}(x_0, y_0) = \phi_\tau(x_0, y_0) + (0, k) \tag{2.2}$$

where the flow $\phi_\tau(x_0, y_0)$ is the flow given by Equation 2.1 for time τ starting at initial condition (x_0, y_0), and the term $(0, k)$ represents a discrete kick of magni-

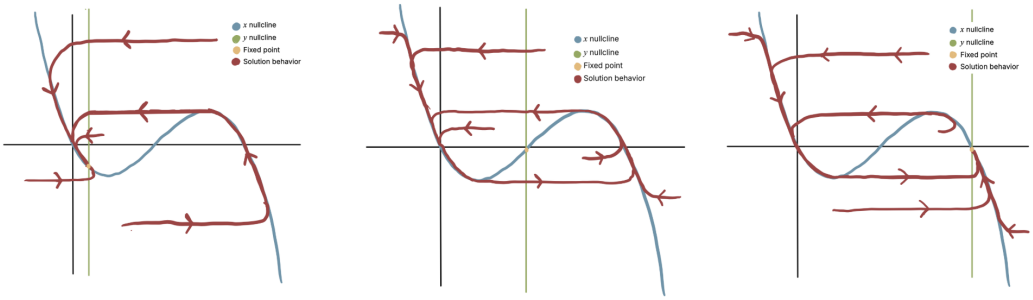

Figure 2.2: Supercritical Hopf bifurcations in the continuous FitzHugh-Nagumo system. The leftmost graph shows solution behavior (red) before the first bifurcation, when the intersection of the nullclines (blue and green) takes place to the left of the local minimum of the cubic nullcline. Solutions asymptotically approach the stable fixed point (yellow) at the intersection of the nullclines. The center graph shows behavior between the bifurcations: a stable limit cycle that follows the cubic nullcline surrounds the unstable equilibrium point at the intersection of the two nullclines, and all solutions are attracted to the stable limit cycle. The rightmost graph shows behavior after the second Hopf bifurcation. A new stable equilibrium point exists at the intersection of the nullclines, which is now to the right of the local maximum of the cubic nullcline, and the limit cycle no longer exists.

tude k applied to the y coordinate only. We can regard the map both as a series of discrete map points, taken in the instant after the kick is applied, and as a continuous flow that can be plotted between these points, with discrete "jumps" that are visible in the time series when kicks are applied.

Chapter 3

Classifying System Behavior Over Parameter Space

We begin our investigation of the flow-kick FitzHugh-Nagumo system by classifying solution behavior over a range of parameter sets. In Section 3.1, we use numerical simulation to find regions in parameter space that are qualitatively similar, ie. have the same stable structures. The boundaries between these regions indicate the presence of bifurcation curves. In Section 3.2, we find and observe patterns in the period count n of solutions at each point (τ, k) in the periodic region that we identified in 3.1. These patterns can characterize certain types of bifurcations.

3.1 Simulation of Periodic and Fixed Point Regions in Parameter Space

The goal of the initial numerical investigation is to find regions in τk-parameter space where a stable fixed point or a stable periodic orbit exists. We

discretize parameter space, creating a grid of points in the range $-5 \leq k \leq 5$ and $1 \leq \tau \leq 50$ with $\Delta k = 0.1$ and $\Delta\tau = 1$. Since it is likely for attracting structures in the flow-kick system to be close to an attracting equilibrium point of the underlying system (12), we use $(x_0, y_0) = (0.2, -0.288)$ as an initial condition to calculate solution trajectories of the flow-kick system. Since we are looking for stable structures, after enough iterations, the trajectories of the maps will closely approach the fixed point or periodic orbit.

Based on previous research (10) and some initial experimentation, we conjecture that the system does not have the potential for bistability, so we use the same initial condition throughout the simulations. At each point in parameter space, we use a "classify" function, described below, to sort the pair of parameter values into categories "fixedpoint", "periodic", or "other".

For the numerical results in this section, we will use the following definitions of fixed points and periodic solutions:

Definition 3.1.1 (Numerical fixed point for a flow-kick map)**.** We define a numerical fixed point for the purpose of this investigation as one where, after 1000 iterations of the map, $|x^* - f(x^*)| < 10^{-4}$. In other words, after a sufficient number of steps, the solution has settled within a margin of error of 10^{-4}.

Definition 3.1.2 (Numerical periodic solution for a flow-kick map)**.** For this investigation, we iterate the map at a parameter set to create a list of map points and search for points that are within 10^{-4} of the final map point. We then count the number of iterations between these repeated points. If the last two intervals are equal and greater than 1, we call the interval n and record the parameter pair as a periodic solution. In other words, we find a solution such that $|f^n(x^*) - (x^*)| < 10^{-4}$ for some particular $n > 1$.

If the point (τ, k) does not meet the criteria for either definition, it is classified as "other". "Other" points tend to be quasiperiodic points that do not settle within the given margin of error after 1,000 iterations. These parameter sets could give chaotic systems, or they could give systems with stable structures that are slower to converge.

The "classify" function uses each pair of parameter values in the lattice to iterate the flow-kick map with initial condition $(x_0, y_0) = (0.2, -0.288)$. Using the `ode15s` solver, it computes the flow over time τ, stops, and adds k to the y coordinate. It then stores the resulting value as a map point and uses the map point as the starting point for the next iteration. After experimentation, it was found that 1000 steps was generally a sufficient amount of time for stable structures to converge within a margin of error of 10^{-4}. After running for 1000 iterates, the above definitions are used to classify the parameter pair as "fixedpoint", "periodic", or "other", using a series of `if` statements that check for fixed points first, then periodic solutions, and then classify as "other" if both checks fail.

Figure 3.1 shows an example time series of each possible classification. Flows are given by colored lines and map points are marked with dots. The red time series represents the "fixed point" category, with map points returning to the same x value after each iteration. The green time series shows a periodic solution, with map points returning to the same value every 3 iterations. The blue time series shows a quasiperiodic solution categorized as "other." Note that map points remain very close to the limit cycle in state space, but do not repeat in a predictable cycle.

Figure 3.2 shows the results of the solution behavior classification in parameter space. Each point on the figure is color-coded to distinguish between fixed points (green), periodic solutions (blue), and other points (yellow). Notably, we

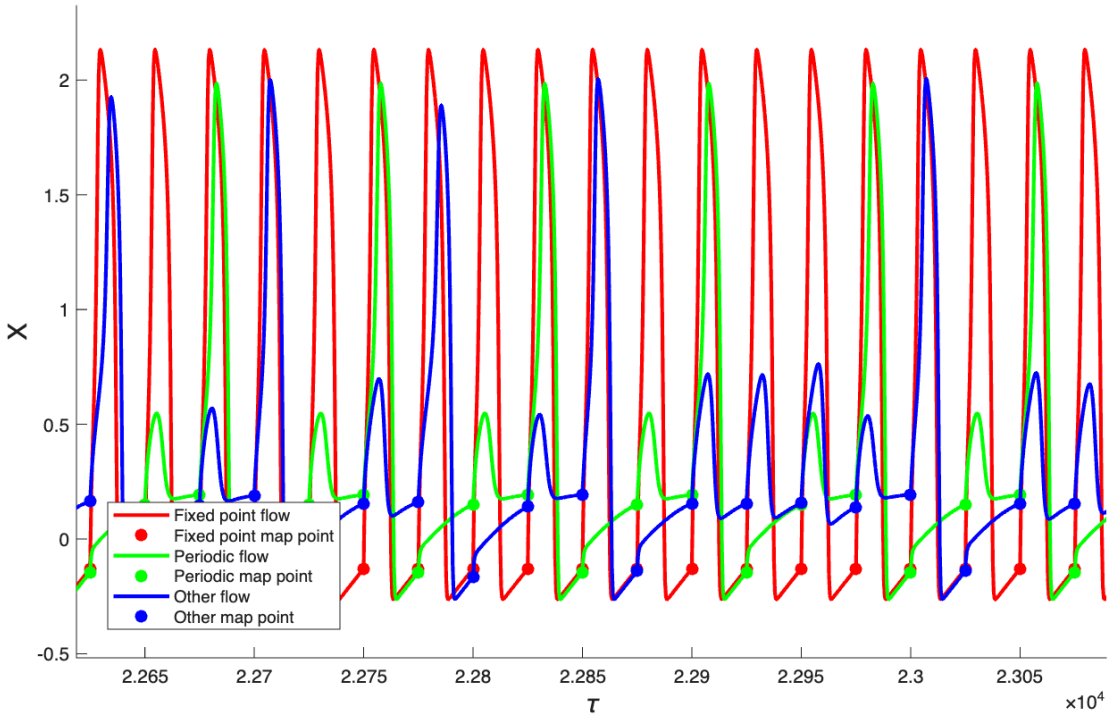

Figure 3.1: Example time series for a numerical fixed point, periodic orbit, and "other" (quasiperiodic) orbit. The fixed point (shown in red) returns to the same x value at every iteration of the map. The periodic orbit (green) repeats the same trajectory every three iterations. The "other" orbit does not exhibit a consistent pattern, but does remain close to the stable limit cycle for a very long period of time. In this example, all solution trajectories were calculated at $\tau = 25$, and the fixed point, periodic orbit, and quasiperiodic orbit were calculated at $k = -1, -0.24$, and -0.25, respectively.

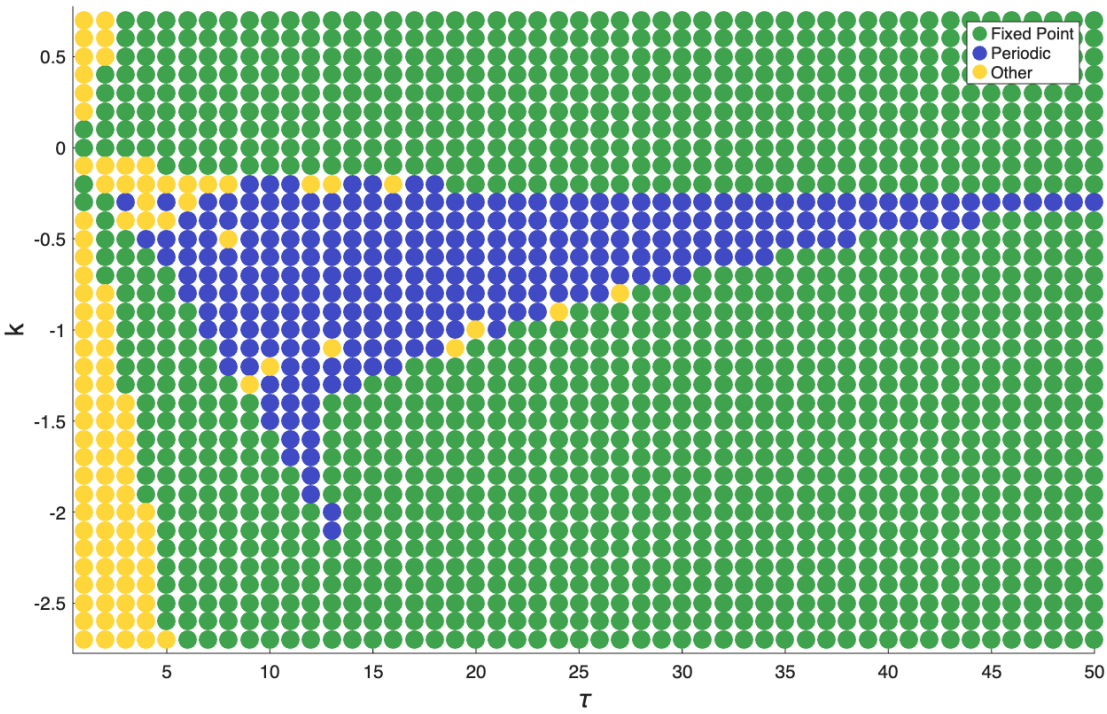

Figure 3.2: Approximation of periodic and fixed point regions in the τk-plane. We observe a region of periodic solutions (blue) located below the $k = 0$ axis with an interesting shape outlined by at least 3 distinct boundary curves. The majority of the plane is comprised of fixed point solutions (green). For some smaller values of τ, as well as some points near the boundary of the periodic region, we see solutions categorized as "other" (yellow). These parameter sets may give chaotic systems, or may give solutions with stable structures that take longer to converge.

see a blue region of periodic solutions below the $k = 0$ axis. We will call this the *periodic region*. The region begins just below the origin and grows in height, encompassing a larger range of k values as τ increases, up to a value of $\tau = 12$. At $\tau = 13$, there are two isolated periodic solutions with k values of -2 and -2.1, then several fixed point solutions between $k = -1.9$ and $k = -1.4$. At $k = -1.3$, the regular shape of the periodic region resumes. For $\tau > 14$, the region begins to narrow vertically, with a long tail close to the $k = 0$ axis stretching on as τ increases. The focus of the rest of our investigation is to analyze and explain the boundaries between the periodic region and the fixed point region, ie. to find and identify bifurcations that occur along these boundaries. The numerical results in the figure support and guide our investigation because they show qualitative differences in solution behavior as parameters are continuously varied.

It has been shown that fixed points and certain types of bifurcations can continue from continuous differential equations to flow-kick maps for sufficiently small flow times (12). For the region in parameter space sufficiently close to the origin, we conjecture that the two supercritical Hopf bifurcations present in the continuous underlying system (Equation 2.1 with $r = 0$) will continue to Neimark-Sacker bifurcations, the map analogue of the Hopf bifurcation. This conjecture is supported by the observed solution behavior: we see the boundary lines between fixed point and periodic behavior emerge from the origin with an average rate of disturbance corresponding to the continuous Hopf bifurcation parameter values. As τ values increase, however, we are no longer able to predict bifurcations based on the behavior of the underlying system. Notably, the curve defining the bottom right boundary of the periodic region is bounded completely away from the $\tau = 0$ axis, meaning that any bifurcation that could explain that boundary is not found in the continuous analogue.

3.2 Classifying Period of Limit Cycles

We use similar numerical techniques to find and chart the period of the stable cycle found at each point in the periodic region. Since some types of map bifurcations, such as the period adding and period incrementing bifurcations, are characterized by specific patterns in the periods of solutions as a parameter is shifted (7), it is useful to be able to observe the patterns of the periodic region as a whole.

To accurately find the periods of solutions in the periodic region of τk-space, we need to change our working definition of a period n solution. More iterations of the map are needed to make sure that the solutions are sufficiently converged, since distances between points on the limit cycle are small. For this reason, we decrease our error tolerance to 10^{-6} and increase the number of iterations to 10,000. For the purpose of this experiment, we define a periodic solution with period n as follows:

Definition 3.2.1 (Numerical period n solution for a flow-kick map)**.** Given a parameter set (τ, k), we iterate the flow-kick map 10,000 times, and take the final map point x_0. We search the list of map points for points within 10^{-6} of x_0. If the interval between such points is the same for the last seven repetitions of the point, we call the solution at (τ, k) a periodic solution with period n, where n is the interval between repetitions.

If this condition is not met, the parameter pair is categorized as not periodic.

Figure 3.3 shows the period n of solutions across the periodic region. Dark blue indicates a lower value of n, and yellow indicates a higher value, with light yellow indicating $n \geq 25$. For better visibility of regions with different periods, values of n are capped at 25. While the majority of n values are under 25, there

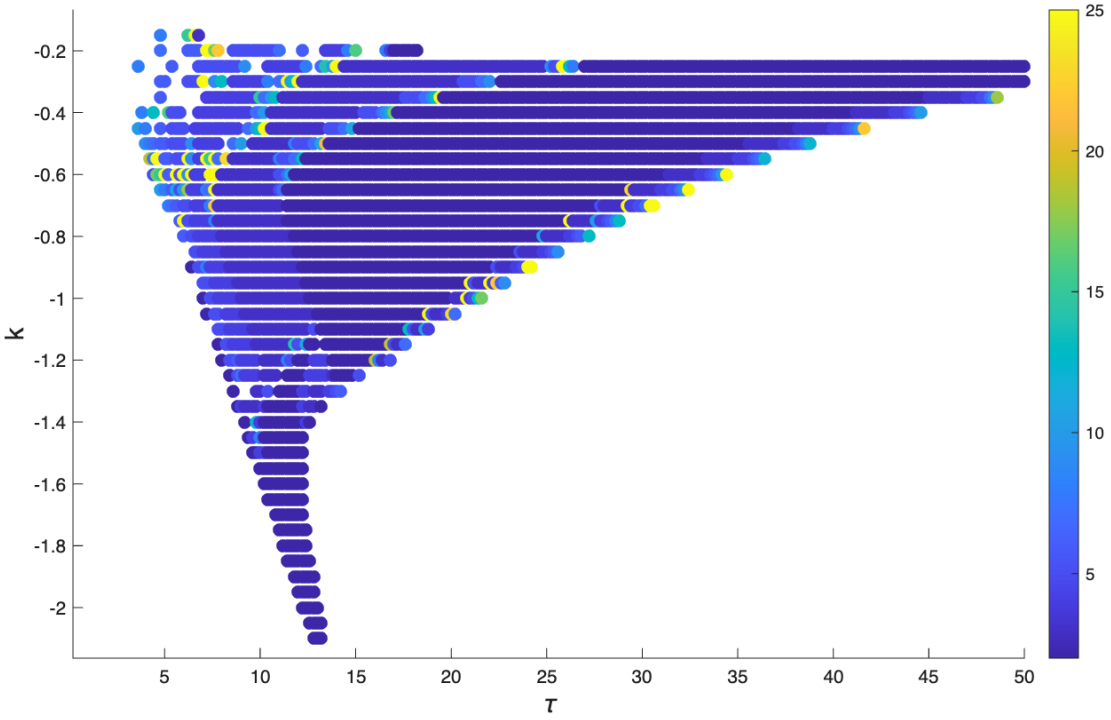

Figure 3.3: Color-coded period count of solutions in the periodic region of parameter space, capped at $n = 25$. Gaps in the plot represent values where solutions do not converge within 10^{-6} after 10,000 iterations. As τ increases, solutions transition through period 4, 3 and 2 (darkest blue) regions separated by areas with higher period counts. Along the bottom right boundary of the periodic region, period count increases rapidly, with several high-period orbits separating the 2-cycle region from the fixed point region.

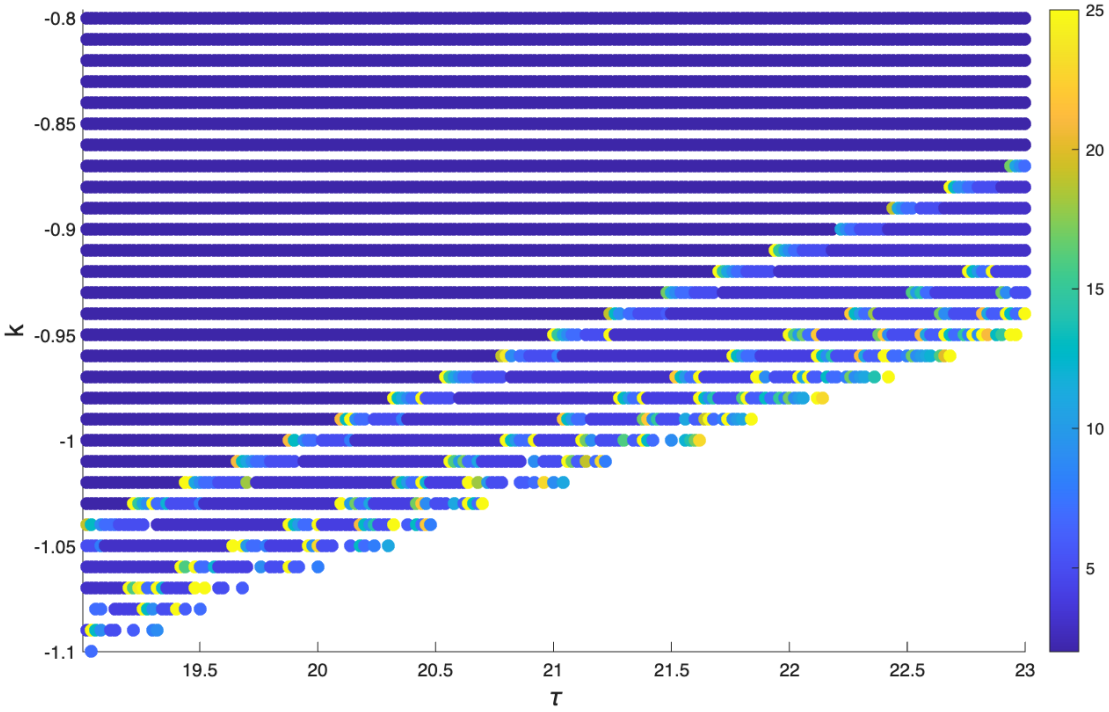

Figure 3.4: Color-coded period count of solutions near the bottom right boundary of the periodic region of parameter space, capped at n=25. Solutions with higher k values and lower τ values have period 2. As solutions approach the edge of the periodic region, the period jumps to a higher value, then decreases to a band of period 3 solutions. The period then increases suddenly again and settles to a narrower band of period 4 solutions. This pattern is repeated for progressively narrowing bands of $n = 5, 6$, and 7, with gaps where the solution does not converge within 10,000 iterations.

are some outliers where n is as high as 290. We see regions of lower n values divided by curves of higher period, starting on the left side of the region with a period 4 region, then a curve of higher period solutions, then a period 3 region, another curve of higher period, and then a period 2 region. The period 2 region is separated from the fixed point region by a narrow region of higher period along the lower right boundary of the periodic region. We will focus our investigation on this boundary.

Figure 3.4 shows the period n of solutions near the lower right boundary of the periodic region. Towards the interior of the region, solutions have period 2. As τ values increase (closer to the boundary), n abruptly increases, to different values at different values of k. As τ continues to increase, n gradually decreases until a band of period 3 solutions is reached. Again, n jumps to much higher values and then gradually decreases to a narrower band of period 4 solutions. This pattern repeats for increasingly narrow bands of period 5, 6, and 7. Gaps occur where no periodic solution exists—these gaps represent solutions that take more than 10,000 steps to converge within the desired tolerance, or where the solution never converges. The τ value at which n jumps seems to vary smoothly as k varies, creating a curve of points just inside the boundary of the region.

In addition, we observe an interesting pattern of behavior in both solutions that converge within the desired tolerance and those that do not. Iterates in an orbit fall along a curve given by $y = -x(x-1)(x-2) + k$ (the cubic nullcline displaced by k units). This can be seen in Figure 3.5. The iterates are clustered into at least two distinct groups along the curve: in this example, we see two groups of points close together below the line $x = 0$ and one group above the line. This pattern is maintained for both periodic and quasiperiodic solutions. This observation is important for the analysis in Chapter 5.

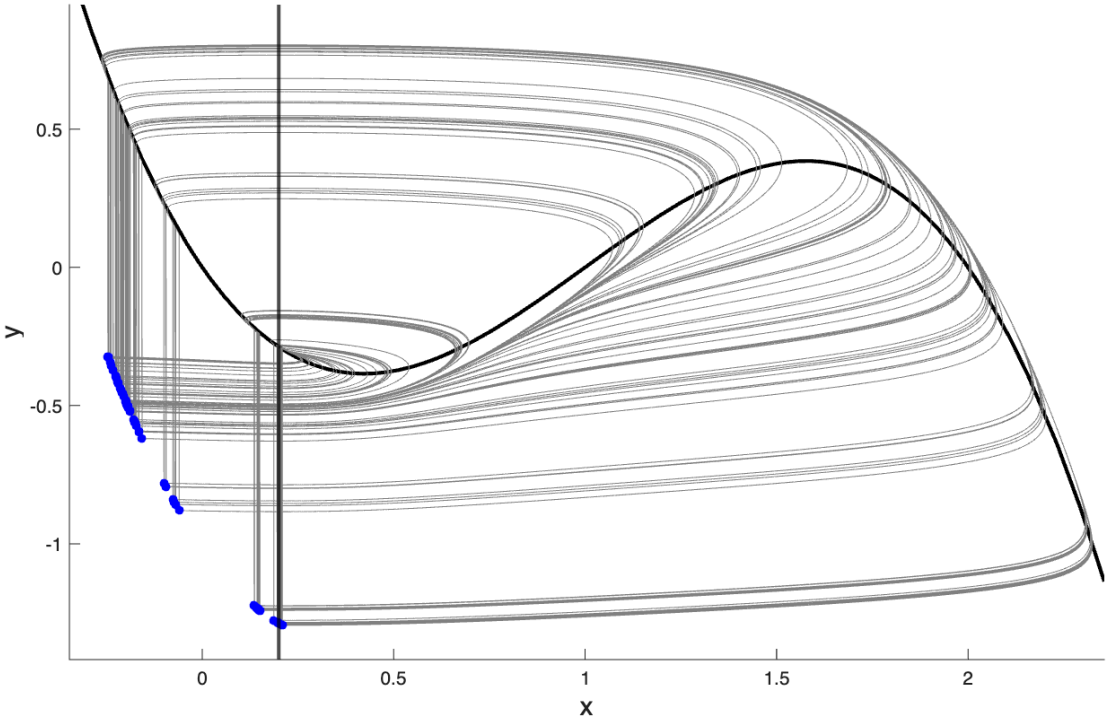

Figure 3.5: Phase portrait at $k = -1, \tau = 20.004$ showing a solution that does not converge to a limit cycle within the desired tolerance. Map points (blue) fall along a curve 1 unit below the cubic nullcline, clustering into at least two distinct groups along the curve.

Chapter 4

Continuation of Bifurcation Curves

The most common approach to finding bifurcation curves in parameter space is to use numerical continuation to find and continue bifurcation points. Whereas in the previous chapter we use observations about solution behavior to find regions separated by various bifurcations, we now attempt to identify the type of bifurcation using continuation. Continuation approximates a bifurcation curve by stepping along the curve of fixed points until we find a bifurcation point. We then step along a curve of bifurcation points to find the bifurcation curve. The curves we find align with some of the boundaries of the regions identified in Chapter 3.

4.1 Continuation: Theory and Implementation

We use the program MatContM that runs through MATLAB to find and continue bifurcations for maps, such as the flow-kick map that we study here. In this section, we will outline the theory behind continuation, as well as the

mechanism by which MatContM finds and continues bifurcation points.

Numerical continuation of fixed points and bifurcation points relies on the Implicit Function Theorem. As parameters are varied continuously, systems vary continuously, and systems close to each other in parameter space are similar enough that curves of equilibrium points and bifurcations can be followed from one system to the next if a small enough step size is used.

Theorem 4.1 (Implicit Function Theorem)**.** Let $x \in \mathbb{R}^n$, and let $\mu \in \mathbb{R}$ be a parameter. Let F be a function $F : \mathbb{R}^n \times \mathbb{R} \to \mathbb{R}^n$. If x_0 is a solution to $F(x_0, \mu_0) = 0$ and $F_x(x_0, \mu_0)$ is nonsingular, then if $|\mu - \mu_0|$ is sufficiently small, there exists a solution x^* to $F(x^*, \mu) = 0$ (3).

In other words, if the new parameter value μ is close enough to the original μ_0, there also exists an equilibrium point near the original equilibrium point. Since we know theoretically that a curve of equilibrium points must exist, we are able to calculate the curve numerically.

MatContM works by varying the value of a chosen parameter slightly and then using a prediction-correction algorithm to find a new fixed point (or bifurcation point) close to that of the previous step. We begin with a "guess" of a point (x, y, τ, k) that we believe to be on or near the curve of fixed points that we are calculating. We then predict the next point on the curve using a tangent vector to the curve. Since MatContM expects a closed-form map, we modify the code to use numerical derivatives, which are approximated using central differences. A correction algorithm is then implemented to correct the guess towards the curve within user-defined tolerances. This process is repeated until a curve of equilibrium points is found. A more detailed description of the process can be found in the MatContM documentation (5; 6).

To find a bifurcation curve, the process is similar. A bifurcation flag is found by checking the eigenvalues along the curve of equilibrium points. When an eigenvalue has the value $|\lambda|= 1$, a bifurcation is flagged. When $\lambda = 1$, a saddle-node bifurcation is flagged. A period-doubling bifurcation is flagged when $\lambda = -1$, and $\lambda\bar{\lambda} = 1$ is a Neimark-Sacker bifurcation (5). Note that the types of bifurcation that MatContM is able to detect are limited to the most common map bifurcations found in smooth, continuous map functions. To follow a bifurcation curve, we begin at the flagged point and use the same prediction-correction algorithm to follow the curve of bifurcation points.

4.2 Bifurcation Curves for the Flow-Kick FitzHugh-Nagumo System

We use MatContM to locate and continue fixed point and bifurcation curves in the flow-kick FitzHugh-Nagumo system. It has been conjectured that Hopf bifurcations in continuous differential equations may continue to Neimark-Sacker bifurcations in flow-kick systems (12). Since two Hopf bifurcations are present in the continuous system with analogous disturbance rates, we hope to observe two corresponding curves of Neimark-Sacker bifurcation in the flow-kick system.

An interesting phenomenon is visible as we continue a fixed point while varying k continuously (Figure 4.1). We fix $\tau = 5$ and set k as the continuation parameter. This is analogous to moving through Figures 3.2 and 4.2 along the vertical line at $\tau = 5$. The position of the fixed point in state space is visible as its position on the x- and y-axes in the figure, and the k labels show the continuous variation in the parameter k. As we move along the curve of fixed points, they

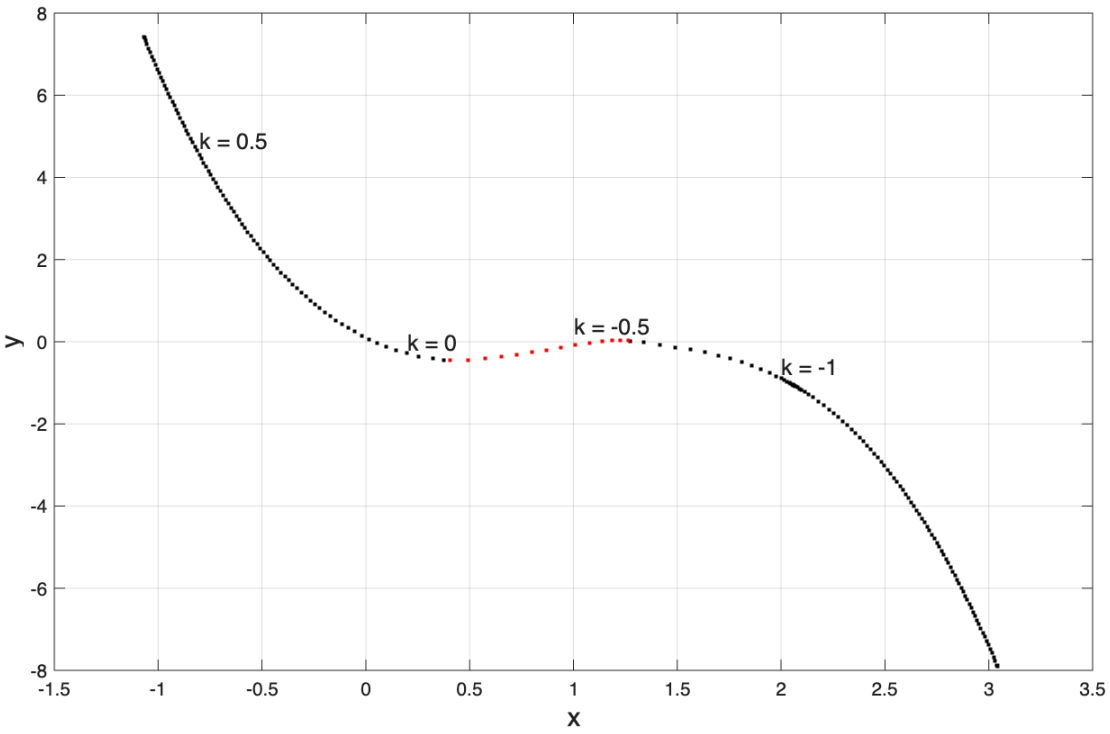

Figure 4.1: Fixed point continuation in k with $\tau = 5$. As k is varied continuously, the state space location of the fixed point also varies continuously. As k is increased, the fixed point goes from stable (black) to unstable (red) at the first Hopf bifurcation, and then back to stable at the second Hopf bifurcation point.

lose stability (turning from black to red) as the first Neimark-Sacker bifurcation is crossed. The unstable fixed point then becomes stable again at the second Neimark-Sacker bifurcation point. This is consistent with the behavior observed in Chapter 3: as we travel along the vertical line at $\tau = 5$, the attracting structure changes from a stable fixed point to a stable limit cycle around an unstable fixed point at the intersection of the nullclines. When the limit cycle disappears at the second Neimark-Sacker bifurcation point, the fixed point regains stability.

Once bifurcation flags have been found on the fixed point curve, we can switch to continuing from those points, varying k and τ simultaneously. We obtain smooth curves of bifurcation points. It is possible for additional bifurcation curves to branch off of the initial curve, which can also be continued. For example, when a Neimark-Sacker curve passes through a 1:2 resonance point (when $\lambda = -1$), a period-doubling bifurcation is flagged. This period-doubling bifurcation point can then be followed to find a curve of period-doubling bifurcation points. Using this method, we obtain the bifurcation curves shown in Figure 4.2.

The figure shows two Neimark-Sacker bifurcation curves (red), which intersect at the origin and extend towards higher τ values. Branching off of each Neimark-Sacker curve are two period-doubling bifurcation curves (black). As τ values increase, continuation eventually fails for both types of bifurcation (predicted bifurcation points fail to converge within specified error bounds in the required number of steps).

Where numerically continued bifurcation curves can be found using MatContM, they outline the periodic region found in Chapter 3. The section of the region closest to the origin is outlined by the two Neimark-Sacker curves, with periodic solutions existing between the Neimark-Sacker bifurcations. The fin-shaped area of the periodic region is outlined to the left by one of the period doubling

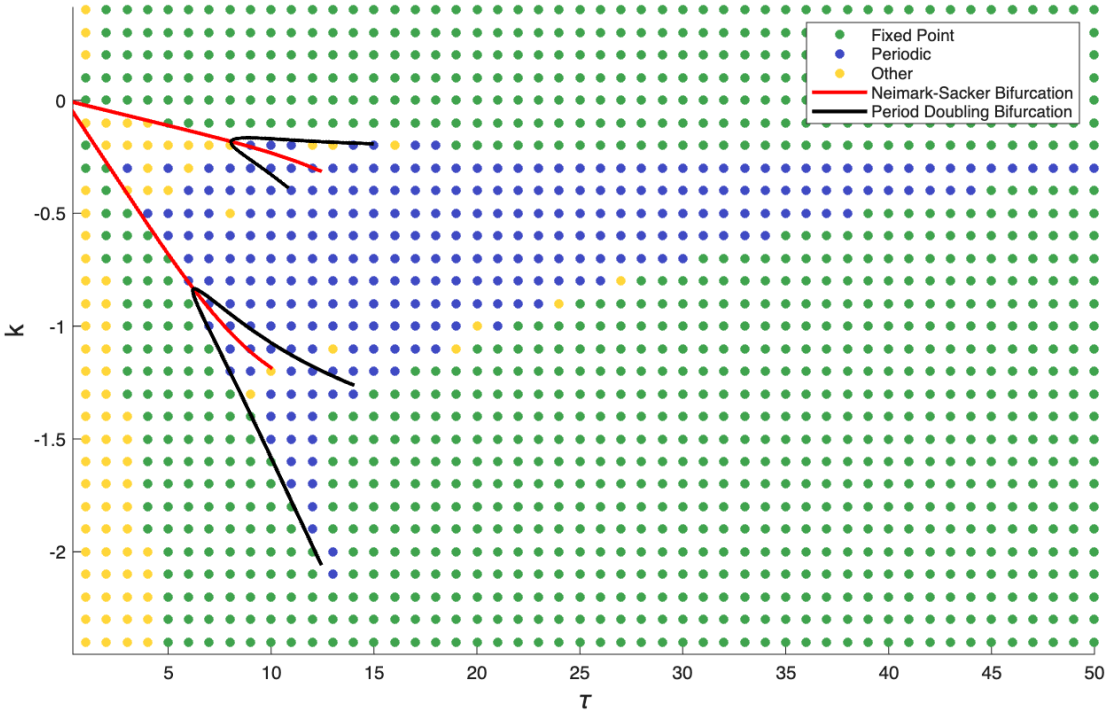

Figure 4.2: Bifurcation curves found using continuation. The flow-kick FitzHugh-Nagumo system exhibits two curves of Neimark-Sacker bifurcations (red), and a curve of period-doubling bifurcations (black) branching off of each Neimark-Sacker curve. These bifurcation curves follow the edges of the periodic region found in Chapter 3. Continuation fails as τ values grow between 10 and 15.

curves. Continuing in the positive direction in k, fixed points in this region become 2-cycles after crossing the curve of period-doubling bifurcations, creating the fin-shaped area of period 2 solutions. The top of the region near $\tau = 10$ is similarly defined by a period-doubling curve.

It has been shown that in flow-kick systems, certain types of bifurcations continue from the fixed points of the underlying system to the corresponding flow-kick systems for sufficiently small τ (12). Here, we conjecture as in (12) that the Neimark-Sacker curves continue from the Hopf bifurcation points in the continuous system. The rates of disturbance r at which the Hopf bifurcations take place correspond to the slope k/τ of the Neimark-Sacker bifurcation curves as $\tau \to 0$. Note that k/τ represents the average rate of disturbance, since it is the magnitude of disturbance divided by the time between disturbances.

Unfortunately, there remains a large area of the boundary of the periodic region that is not able to be explained by the numerically continued bifurcation curve. This region is also bounded away from the k-axis, meaning that bifurcations present in the continuous system are very unlikely to explain behavior in this region. We explore this region using other techniques in Chapter 5.

Chapter 5

Period Adding Bifurcations

Using numerical continuation, we identified bifurcation curves that form the top and bottom left boundaries of the region in parameter space where periodic solutions exist. However, numerical continuation fails for larger values of τ, so we employ other techniques to observe solution behavior for larger values of τ and form a conjecture about bifurcations that exist at these values. We use numerical simulation to create bifurcation diagrams in both k and τ in order to observe the behavior of stable structures near the boundary. We also use symbolic dynamics to compare the behavior of our system to known bifurcation types described in the literature: the period adding and period incrementing bifurcations (7).

5.1 Bifurcation Diagrams

We begin by producing bifurcation diagrams in k or τ showing solution behavior in state space. We aim to observe changes in stable structures when crossing the boundary from the fixed point region to the periodic region. We cross the boundary in two directions, horizontally by varying τ and vertically by

varying k. Data for the diagrams is calculated using the numerical technique described in Section 3.2, where the flow-kick map is iterated for 10,000 steps and solutions must converge within a margin of error of 10^{-6}. Each stable structure found is color-coded according to the period of the solution at that value, with values over 25 capped for readability.

5.1.1 Bifurcation Diagrams in τ

Figures 5.1a and 5.1b show the behavior of stable structures (fixed points and periodic orbits) in state space as τ is varied with a step size of 0.01 between 19.5 and 22, with a constant $k = -1$. Figure 5.1a shows the x values of the stable structures at each value of τ, and Figure 5.1b shows the y values. As τ decreases, crossing the boundary of the periodic region, the stable fixed point at approximately $(x, y) = (-0.2, -0.5)$ becomes a stable limit cycle between $\tau = 21.63$ and $\tau = 21.64$.

Periodic orbits tend to have iterates that cluster in two regions: one near $(x, y) = (-0.2, -0.5)$, which is the location in state space of the fixed point at $(\tau, k) = (22, -1)$, and the other near $(x, y) = (0.2, -1.3)$, which corresponds to the fixed point that exists for larger values of k. There are some gaps where solutions do not converge to the specified margin of error within 10,000 steps—these solutions behave similarly to the quasiperiodic solutions from Section 3.2. These gaps tend to cluster near the τ values where the attracting structure changes from a fixed point to a limit cycle. This behavior is expected, since solutions converge more slowly near bifurcation points. As τ decreases, we observe lower periods and longer intervals where the period remains constant.

As is shown in Figure 3.4, the majority of the periodic region near the fixed-

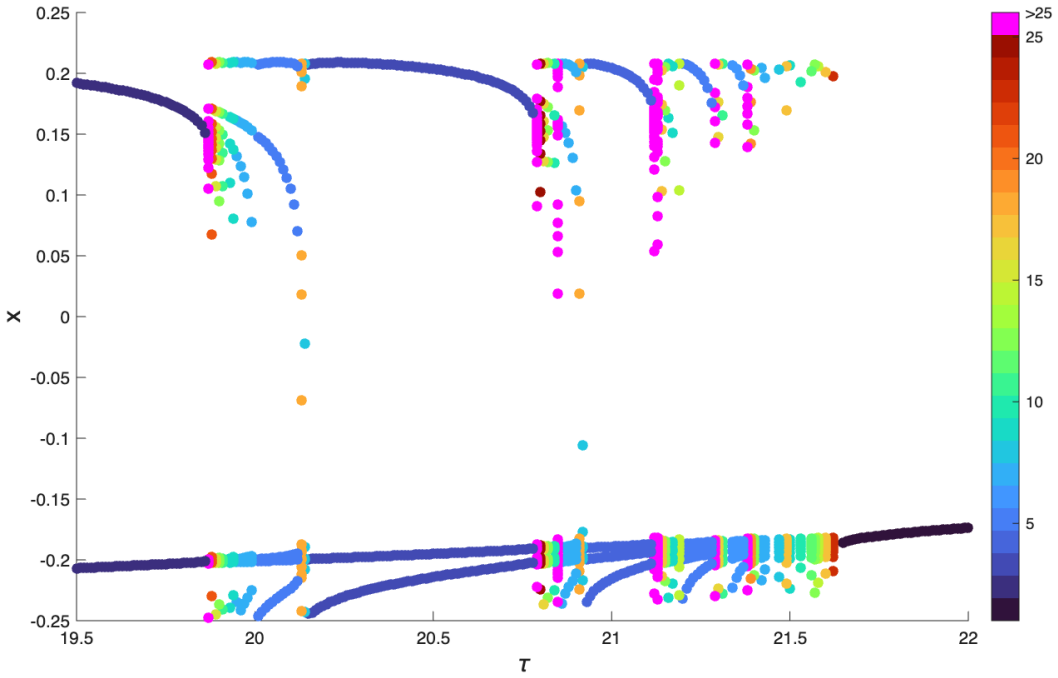

(a) Bifurcation diagram in τ and x

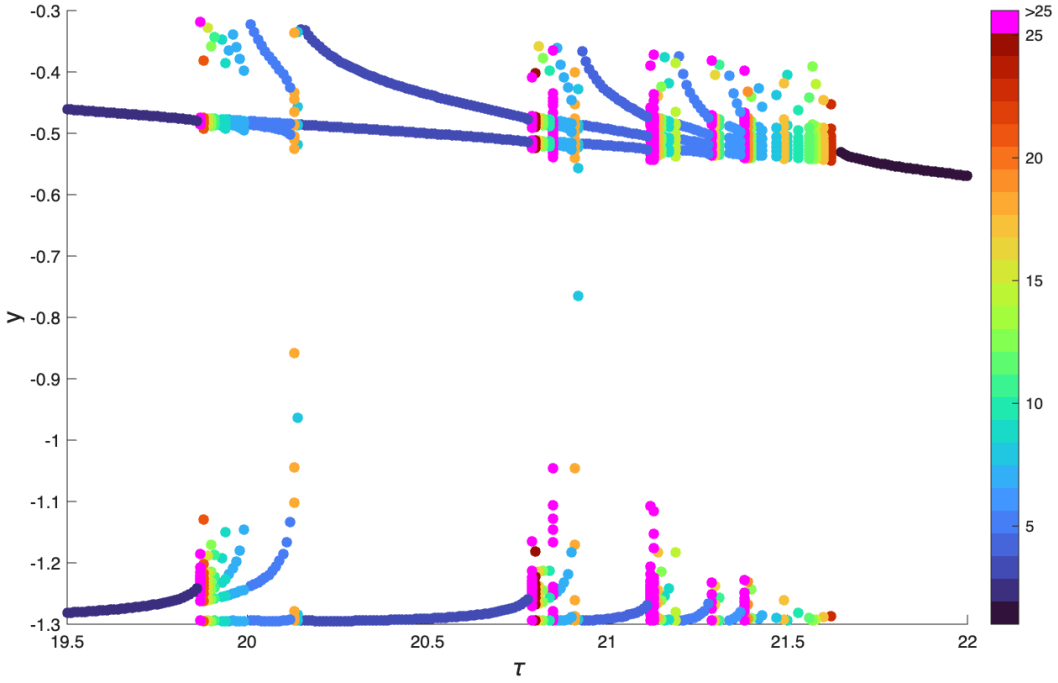

(b) Bifurcation diagram in τ and y

Figure 5.1: Bifurcation diagrams in τ with $k = -1$. Color represents the period of stable structures, with lower periods dark blue and higher periods red and pink. As τ increases, we observe a period incrementing structure, with intervals of constant period interrupted by regions of higher-period orbits. At $\tau = 21.64$, the system transitions to a fixed point.

point boundary is populated by 2-cycles. Figure 5.1 shows the behavior of stable structures from the edge of the 2-cycle region to the boundary of the periodic region. As τ increases, the points on the 2-cycle move towards each other in state space, and then transition to a 37-cycle. The period then continuously decreases for a brief interval before transitioning to an 18-cycle. After the 18-cycle, the system transitions to a 3-cycle for a relatively long interval of τ values.

Continuing to increase τ, we observe a region of high period counts, and then a shorter interval of τ values where a 4-cycle exists. The 4-cycle then also disintegrates into a region of higher period counts. This pattern of an interval of an n-cycle and then a band of higher period counts repeats for $n = 5, 6, 7, 8, 9, 10$, at which point periods begin to climb rapidly right before the transition to a fixed point. This incrementing pattern is notable because of its similarity to the period incrementing bifurcation scenario described in the literature (7).

5.1.2 Bifurcation Diagrams in k

Figures 5.2a and 5.2b show the behavior of stable structures for $-1 < k < -0.001$, where k is varied with a step size of 10^{-3} and $\tau = 25$. From $k = -1$ to $k = -0.878$, we observe a fixed point located at approximately $(x, y) = (-0.13, -0.6)$. As k increases, we cross the boundary from the fixed point region to the periodic region, transitioning from a fixed point at approximately $(x, y) = (-0.13, -0.6)$ to a periodic orbit with period greater than 25 at $k = -0.877$.

As k continues to increase, the period decreases in an incrementing pattern similar to the one observed in Figure 5.1. We see a sequence of intervals where the period decreases by 1 interspersed with intervals of variable higher period. For example, the system transitions from an interval of 5-cycles to an interval

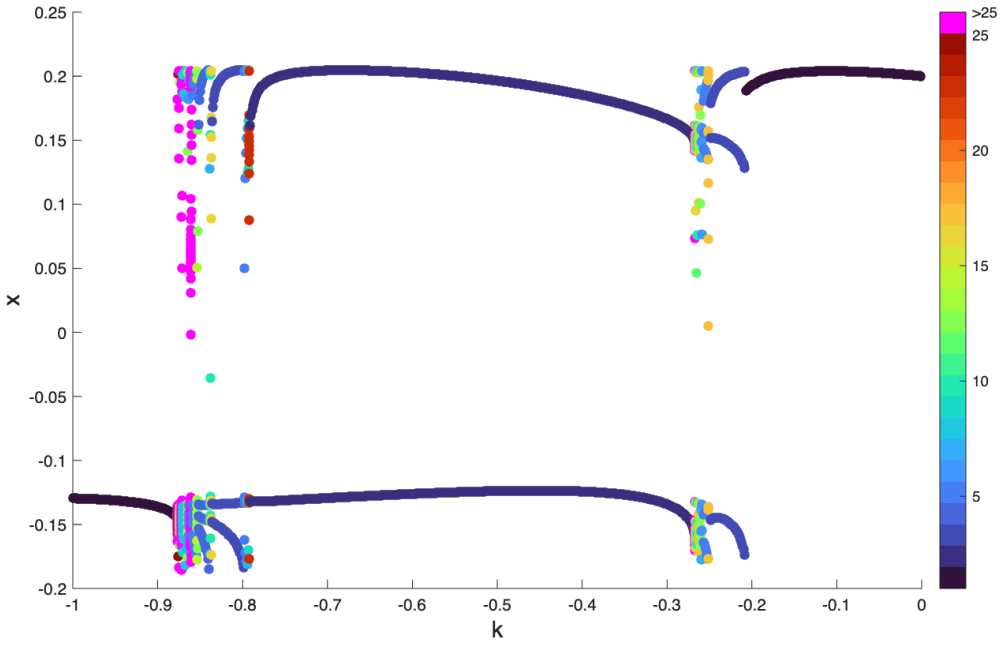

(a) Bifurcation diagram in k and x

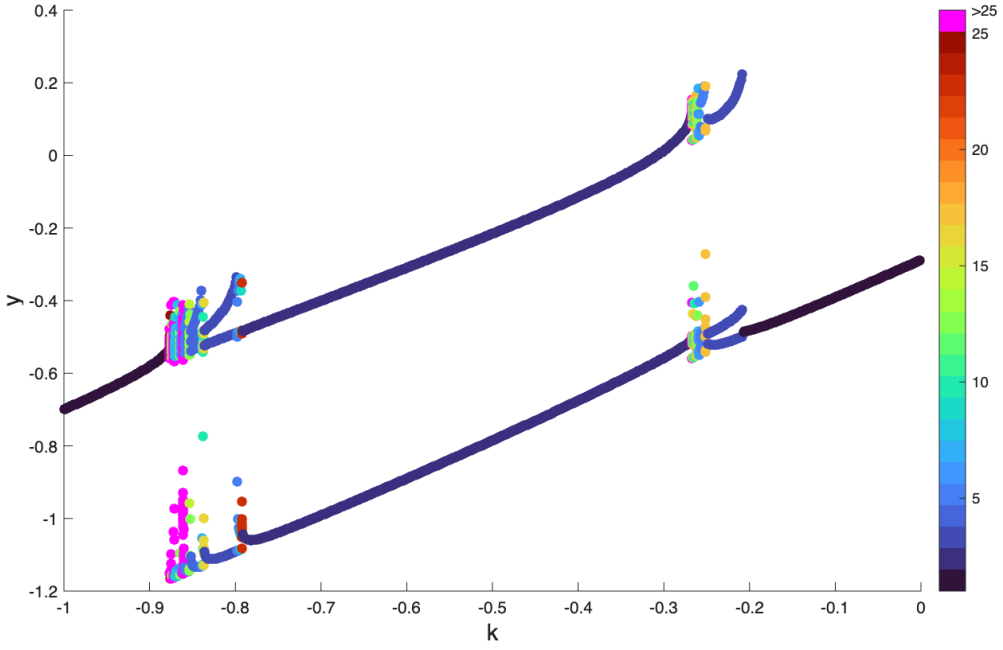

(b) Bifurcation diagram in k and y

Figure 5.2: Bifurcation diagrams in k, with $\tau = 25$. Color represents the period of stable structures, with lower periods dark blue and higher periods red and pink. We observe a transition from a fixed point near $(x, y) = (-0.13, -0.6)$ to an interval of periodic solutions displaying a decreasing incrementing pattern. We transition to a long interval of period 2 solutions, then an interval of higher-period solutions, then an interval of period 3 solutions, before transitioning to a fixed point near $(x, y) = (0.2, -0.4)$.

of higher period solutions to a slightly longer interval of 4-cycles. This pattern continues until an interval of 3-cycles is reached.

We then observe a small interval of higher periodic solutions before the system transitions to a very long interval of 2-cycles from $k = -0.791$ to $k = -0.268$. At $k = -0.267$, we see another solution with a period count greater than 25. Periods then begin to decrease in a similar incrementing pattern, with bands of constant period n interrupted by small regions of higher period. As n decreases, the lengths of the intervals of solutions that have period n increase.

At $k = -0.209$, we cross the boundary from the periodic region to the fixed point region, transitioning from an interval of 3-cycles to a fixed point near $(x, y) = (0.2, -0.5)$.

5.1.3 Comparison to Bifurcations in Nonsmooth Systems

In our bifurcation diagrams, we observe two interesting behaviors. First, we notice an incrementing structure in the period of our periodic solutions. Second, iterates of cycles move through state space, connecting the fixed points on either side of the periodic region. These behaviors are indicative of the period adding and period incrementing bifurcations.

The *period incrementing bifurcation* is characterized by regions of n-periodic and $(n+1)$-periodic solutions separated by regions of bistability where n-periodic and $(n+1)$-periodic solutions coexist. As this pattern repeats across a range of parameter values, n increases by one at each new interval of periodic solutions (7).

The *period adding bifurcation* is characterized by regions in parameter space of periodic orbits with period count given by the addition of the period counts of

the two adjacent regions. For example, a region of period 5 solutions might exist between a region of period 3 solutions and a region of period 2 solutions. The period adding bifurcation also has the property that the proportion of periodic points in a particular area of state space—for example, near a particular fixed point—is both monotonically increasing and locally constant almost everywhere in a number of discrete regions. In other words, as the parameter is varied, iterates transition from being clustered near the state space location of one fixed point to being clustered near a different fixed point. We will define this concept more precisely in Section 5.2.

In our bifurcation diagrams in τ (Figure 5.1), we observe a structure similar to the period incrementing bifurcation. There exist intervals of constant period n that transition to regions of a distinct and different type of behavior before transitioning to a region of period $(n + 1)$ solutions. As the period increases, the length of the corresponding interval in τ decreases. From our observations, our system does not have the potential for bistability, so we lack the regions of bistability between periodic intervals. Instead, the regions between the distinct intervals of period n show period counts that are very high and vary quickly, and some contain gaps where solutions do not converge to a periodic orbit within 10,000 iterations.

Our bifurcation diagrams in k exhibit an interesting similarity with the period adding bifurcation. On each side of the periodic region, there exists a fixed point in a different region in state space. We observe that periodic orbits tend to have iterates that cluster in two distinct regions of state space, with each region located near one of the fixed points. For lower k values, iterates of the cycle cluster in one region, with very few points in the other region. As k increases, iterates slowly transition to clustering in the other region, with very few remaining in

the first region. This clustering is examined using symbolic dynamics in the next section.

5.2 Symbolic Dynamics

In the previous section, we observed that the solutions near the boundary of the periodic region follow a period incrementing structure. As τ increases, we see intervals of constant period interrupted by regions of other interesting behaviors as described in Section 5.1.1. At each subsequent interval the period increases by 1. We also observe that as k increases, the majority of periodic points shift from being concentrated near the fixed point at $(x, y) = (-0.125, -0.6)$ to being concentrated near the fixed point at $(x, y) = (0.2, -0.4)$. This is consistent with the structure of a period adding bifurcation. In this section, we will investigate these similarities further using symbolic dynamics. The relationship between the period adding/incrementing bifurcations and symbolic dynamics is explored in the SIAM review paper by Granados et al. (7). We will begin by providing the necessary definitions to understand our work, and establish the partition that we will use to divide phase space. We will discuss our findings and compare them to the results presented in the literature. The full data tables are provided in the appendices.

5.2.1 Background and Definitions

Using symbolic dynamics, we are able to study characteristics of our system in a simplified way. We partition phase space into two regions and assign a symbolic value to each region. We can then examine solution trajectories in terms of the simplified sequence of symbols, rather than complex trajectories.

This approach reveals common patterns with established bifurcation types.

We begin by providing definitions that we will use to construct our data.

Definition 5.2.1 (Symbolic sequence of a trajectory)**.** Given a point (x_0, y_0) in phase space, we associate its trajectory

$$(x_0, y_0), G_{\tau,k}(x_0, y_0), G^2_{\tau,k}(x_0, y_0), G^3_{\tau,k}(x_0, y_0)...$$

with a symbolic sequence given by

$$a(x_0, y_0), a(G_{\tau,k}(x_0, y_0)), a(G^2_{\tau,k}(x_0, y_0)), a(G^3_{\tau,k}(x_0, y_0))...$$

where:

$$a(x) = \begin{cases} R & \text{if } x \geq -0.1 \\ L & \text{if } x < -0.1 \end{cases}$$

(7)

The value of $x = -0.1$ was chosen as the partition because of the distinct groups of periodic points in phase space apparent in the bifurcation diagrams (see Figures 5.1a, 5.2a).

For this experiment, we will focus on the symbolic sequences associated with periodic orbits. The symbolic sequence associated with a periodic solution of period n also has length n. Note that since we may start recording the symbolic sequence of a periodic orbit at any point on the orbit, each periodic solution can be represented as a symbolic sequence in n different ways, which can be obtained as cyclic permutations of the symbolic sequence.

For convenience, we denote blocks of the same symbol using exponents. For example, the sequence $LLLLRLLLR$ is denoted L^4RL^3R.

In order to represent symbolic sequences in a standardized way, we introduce lexicographical ordering. We let $L < R$ so that for two sequences $(x_1x_2...), (y_1y_2...)$:

$$(x_1x_2...) < (y_1y_2...)$$

if and only if $x_1 = L$ and $y_1 = R$ or $x_1 = y_1$ and there exists some $j > 1$ such that $x_i = y_i$ for all $i < j$, $x_j = L$, and $y_j = R$ (7).

Given a periodic symbolic sequence, we will represent it using its minimal sequence. This is the cyclic permutation of the sequence lowest in the lexicographical order.

An important characteristic of a symbolic sequence is the ratio of the number of each symbol present to the total length of the sequence. We represent this characteristic using the η number.

Definition 5.2.2 (η number for a symbolic sequence)**.** For a symbolic sequence of length n, let r be the number of times that the symbol R appears in the sequence. Then the η number for that sequence is $\frac{r}{n}$.

For this experiment, we use solution trajectories calculated for the bifurcation diagrams in Section 5.1. We begin at an arbitrary point on the converged periodic orbit, and use MATLAB to categorize the point as L or R based on its position in state space. We then proceed along the orbit and categorize each point until we have obtained a symbolic sequence of length n. We calculate the η number by counting the instances of symbol R and dividing by n. Minimal sequences are then found manually.

5.2.2 Findings and Comparison to Existing Results

For a detailed exploration of the symbolic dynamics of period adding and period incrementing bifurcations, we refer to the SIAM review paper by Granados et al. (7).

The period adding bifurcation is characterized by the relationship between neighboring intervals of parameter values where each interval is composed of solutions with constant period. The period count n of solutions in one interval are given by the addition of those in neighboring intervals: for example, a region of period 5 solutions might exist between neighboring regions of period 2 and period 3 solutions. Additionally, the symbolic sequences of solutions in a region are given by the concatenation of neighboring regions—a region of periodic solutions with the minimal symbolic sequence L^3RL^2R would exist between regions with minimal sequences L^3R and L^2R.

Another important characteristic of the period adding bifurcation is related to the η number, which follows a devil's staircase.

Definition 5.2.3 (Devil's staircase)**.** A *devil's staircase* is a function that is monotonically increasing and locally constant everywhere except for a Cantor set of measure zero (7).

In other words, the proportion of points on a particular side of the phase space partition increases monotonically as a parameter is varied, and is locally constant in a number of discrete regions with their own distinct symbolic sequences.

The period incrementing bifurcation is characterized by regions of periodic solutions separated by regions of bistability where solutions with the period of both neighboring regions coexist. Symbolic sequences for all solutions take the

form L^iR, where i is some positive integer. There are no sequences containing more than one R symbol. In each subsequent periodic region, the period count n increases by one. In other words, consecutive regions have the pattern L^iR, bistability between L^iR and $L^{i+1}R$, and then $L^{i+1}R$.

Figures 5.3a and 5.3b show the value of η as τ and k are varied. Areas highlighted in red are points that do not follow the devil's staircase structure, ie. break the monotonicity. These areas also have atypical symbolic sequences and may be due to numerical error caused by the sensitivity of the system — further work is needed to explain these findings. Areas highlighted in gray represent parameter values where no periodic orbit exists. When a relatively long interval of a particular symbolic sequence exists, the sequence is labeled.

In Figure 5.3a, which shows the η number as τ is varied, we observe a devil's staircase typical of the period adding bifurcation. The η number is locally constant almost everywhere, and is also monotonically decreasing with the exception of one point (red). The symbolic sequence at this point is atypical, and iterates of the orbit at this point lie extremely close to our chosen partition. Note the higher concentration of gray areas as τ approaches the value at which the system transitions to a fixed point. As we approach the bifurcation point, solutions are slower to converge, meaning that some stable structures may not converge within the given number of iterations.

In Figure 5.3b, which shows the η number as k is varied, we observe η increasing quickly over a series of small intervals for lower values of k. As k increases, we see longer intervals with sequences L^3R and L^2R, and a long interval of sequence LR. We then see some short intervals, an interval of $LRLR^2$, and an interval of LR^2. Notably, for the majority of k values, η also follows a devil's staircase, with η locally constant almost everywhere and monotonically increasing

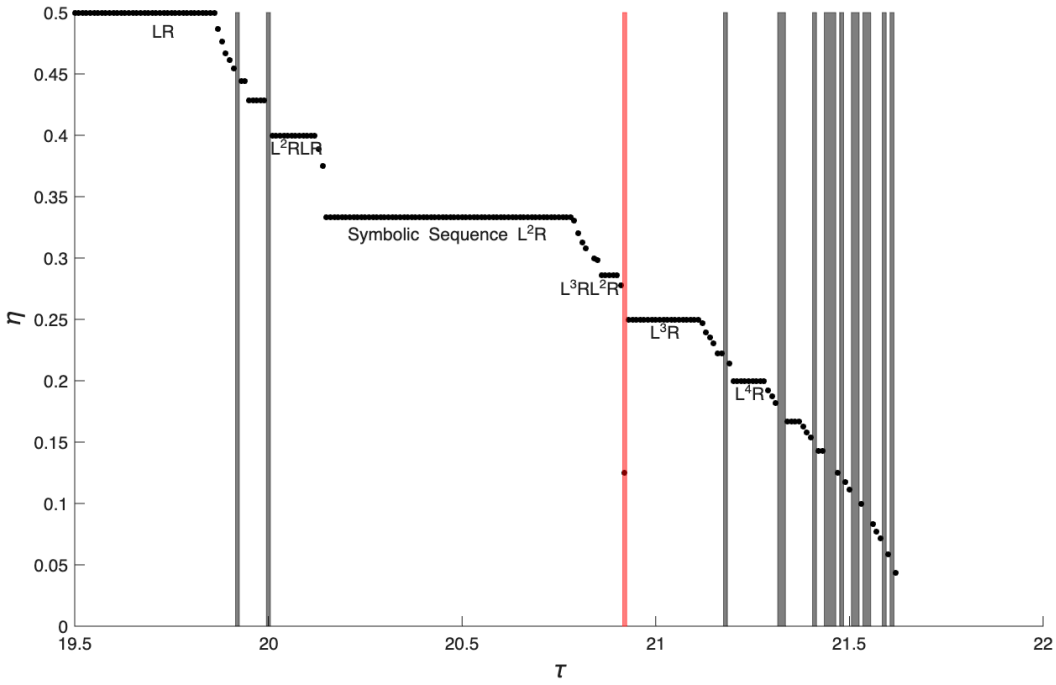

(a) τ vs. η

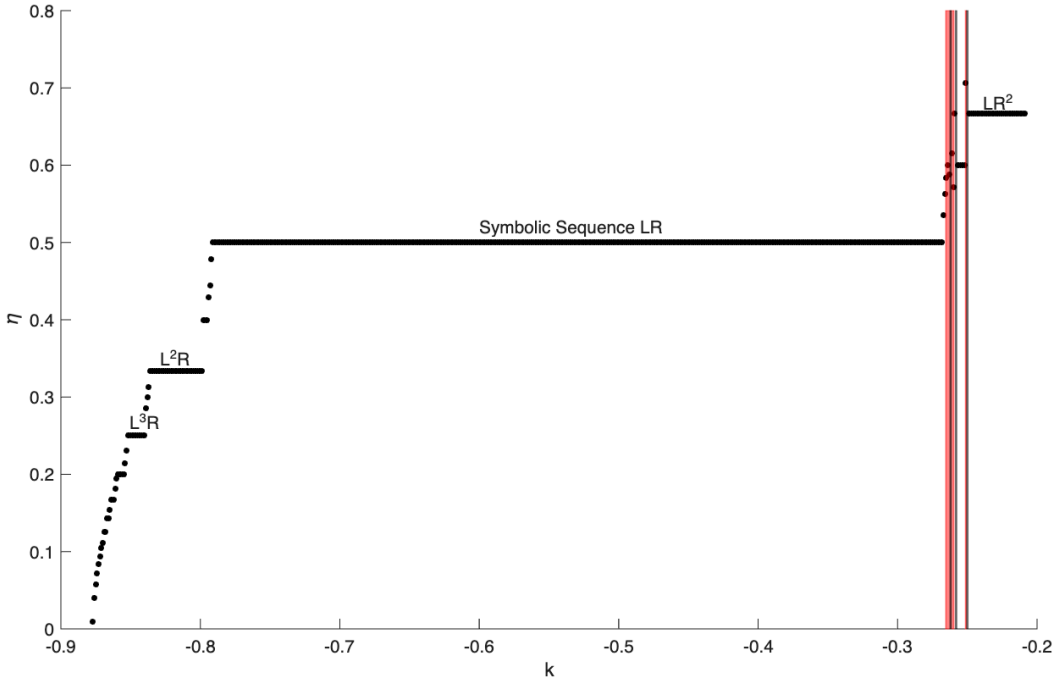

(b) k vs. η

Figure 5.3: Parameters τ and k vs. η number. Gray highlights represent parameter values where the system does not converge to a stable structure. The η number follows a devil's staircase, with the exception of a small set of parameter values where η is not monotonically increasing/decreasing. These values are highlighted in red.

except for a small set of points. Similarly to Figure 5.3a, parameter values which do not follow the devil's staircase structure have atypical symbolic sequences and require further investigation.

Figures 5.4a and 5.4b show the period count n as the parameters τ and k are varied. In both figures, long intervals of the same symbolic sequence are labeled, and areas of higher period (as observed in Figures 5.1 and 5.2) are highlighted in gray.

In Figure 5.4a, we observe an incrementing structure where regions of period n and period $(n+1)$ are separated by regions of higher period count. Notably, the symbolic sequences of these incrementing blocks are all of the form L^iR, as in the period incrementing scenario in (7). A major difference is the presence of cycles with the symbolic sequence $L^{i+1}RL^iR$ (or $L^{i+1}R(L^iR)^n$) rather than bistability between L^iR and $L^{i+1}R$, as in the literature. This is a phenomenon to be explored in future work. Notably, there exist intervals within the gray regions with symbolic sequences given by the concatenation of the neighboring regions, as in the period adding scenario. Other sequences in the gray region tend to be given by $L^{i+1}R(L^iR)^n$, where L^iR and $L^{i+1}R$ are the sequences of neighboring incrementing blocks.

Table 5.1 demonstrates the pattern of an interval of symbolic sequences of the form $L^{i+1}R$, an interval of sequences that are a combination in some form of $L^{i+1}R$ and L^iR, and an interval of sequences L^iR. This pattern is typical of the gray intervals in Figure 5.4a.

For example, for the interval $21.34 \leq \tau \leq 21.37$, we have the sequence L^5R. In the neighboring interval $21.42 \leq \tau \leq 21.43$, we have the sequence L^6R. The region in between has varying sequences given by the concatenation of the symbolic block L^6R and various numbers of occurrences of the symbolic block L^5R.

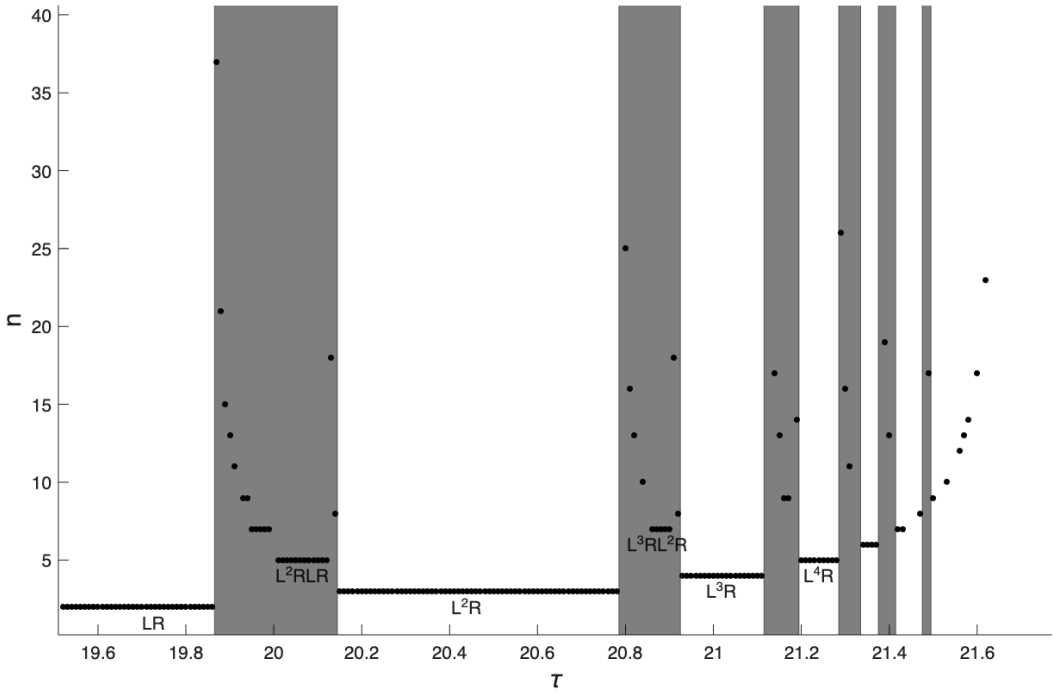

(a) τ vs. n

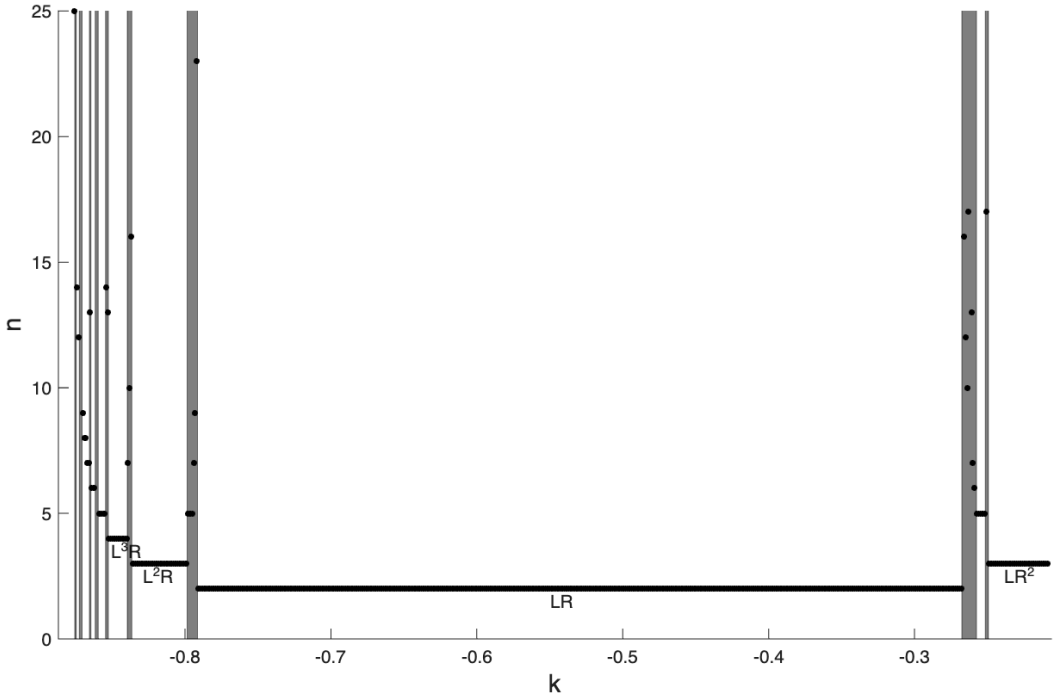

(b) k vs. n

Figure 5.4: Parameters τ and k vs. period count n. Areas of higher period between incrementing blocks are highlighted in gray. Some higher values of n have been excluded for visibility. We observe an incrementing structure in both figures, with symbolic sequences in the gray areas given by concatenation of sequences of neighboring incrementing blocks.

τ	Minimal Sequence	r	n	η number
21.43	L^6R	1	7	0.1428571429
21.42	L^6R	1	7	0.1428571429
21.4	L^6RL^5R	2	13	0.1538461538
21.39	$L^6RL^5RL^5R$	3	19	0.1578947368
21.38	$L^6RL^5RL^5RL^5RL^5RL^5RL^5R$	7	43	0.1627906977
21.37	L^5R	1	6	0.1666666667
⋮	⋮	⋮	⋮	⋮
21.34	L^5R	1	6	0.1666666667

Table 5.1: Example symbolic sequences of higher period region between incrementing blocks as τ is varied. Note that higher-period symbolic sequences take the form $L^{i+1}R(L^iR)^n$, where L^iR and $L^{i+1}R$ are the sequences of neighboring incrementing blocks.

The pattern of sequences given by the concatenation of neighboring sequences is characteristic of the period adding scenario in (7).

Figure 5.4b shows the period count of solutions at varying k values. We see a similar incrementing structure for lower k values, with the period increasing as k decreases. In addition, we see the period increase for higher k values, breaking the pattern of decreasing by 1 each interval. Similarly to Figure 5.4a, for the regions between the incrementing intervals, the symbolic sequences are given by concatenation of neighboring regions, with the lower-period sequence often appearing more than one time. This pattern is exemplified in Table 5.2.

From our symbolic dynamics data, we see strong evidence that the period adding or period incrementing bifurcation types exist in this system. Further work is needed to verify these bifurcation types by analytical conditions.

k	Minimal Sequence	r	n	η number
-0.852	L^3R	1	4	0.25
⋮	⋮	⋮	⋮	⋮
-0.84	L^3R	1	4	0.25
-0.839	L^3RL^2R	2	7	0.2857142857
-0.838	$L^3RL^2RL^2R$	3	10	0.3
-0.837	$L^3RL^2RL^2RL^2RL^2R$	5	16	0.3125
-0.836	L^2R	1	3	0.3333333333
⋮	⋮	⋮	⋮	⋮
-0.799	L^2R	1	3	0.3333333333

Table 5.2: Example symbolic sequences of higher period region between incrementing blocks as k is varied. Similarly to Table 5.1, higher-period symbolic sequences take the form $L^{i+1}R(L^iR)^n$.

Chapter 6

Conclusion

Flow-kick maps exhibit surprisingly interesting structures in comparison to generic continuous maps. We investigate the extent to which stable structures and bifurcations continue from the continuous FitzHugh-Nagumo system to the flow-kick analogue. Using numerical simulation to find stable structures at various parameter sets, we discover a region of periodic solutions in τk-parameter space that is outlined by at least three distinct boundary curves, one of which is bounded away from the continuous system at $\tau = 0$ (Chapter 3).

Building on this work, we use MatContM to find and numerically continue bifurcation curves in parameter space that align with the boundaries of the periodic region (Chapter 4). We find two Neimark-Sacker bifurcation curves that align respectively with the top and bottom-left boundaries. This finding provides further evidence towards the conjecture put forth in (12) that Hopf bifurcations can continue from a continuous differential equation to the analogous flow-kick system for small enough τ. Future research in this area could include a proof of the continuation of Hopf bifurcations to Neimark-Sacker bifurcation curves.

Notably, MatContM continuation fails for larger τ values, and the bottom-

right boundary of the periodic region is not explained by bifurcation curves found using numerical continuation. In order to identify a bifurcation at this boundary, we use numerical simulation to create bifurcation diagrams in both k and τ (Section 5.1). We observe a period incrementing structure as τ is varied, with intervals of solutions with constant period interrupted by regions of higher period. The period count of each successive interval increases by 1. This is reflective of the period adding or incrementing bifurcation structure.

To solidify our evidence for this type of bifurcation structure, we introduce symbolic dynamics. We observe a structure of intervals of sequences L^iR, where i increases by 1 at each successive interval (Section 5.2). In the regions between these intervals, where solutions have higher period, symbolic sequences are given by the concatenation of the sequences of neighboring intervals. Additionally, for continuations in both k and τ, the η number is locally constant almost everywhere and monotonically increasing, with the exception of a small number of atypical points which may be caused by numerical error due to the sensitivity of the system. This evidence points to the existence of a period adding or period incrementing bifurcation in our system. This is especially notable because these bifurcation structures have been previously observed only in piecewise-smooth discontinuous systems. However, while we have found strong evidence towards this conjecture, further work is necessary to formalize this observation and to understand why these types of bifurcations are present in this system. Moreover, the concatenation observed in the regions between the incrementing intervals does not follow descriptions in the literature, which could warrant further investigation. Nonetheless, we believe that we have identified a period adding bifurcation in a novel class of systems.

Appendix A

Symbolic Sequences with Varying τ

τ	Minimal Sequence	r	n	η number
21.62	$L^{22}R$	1	23	0.04347826087
21.6	$L^{16}R$	1	17	0.05882352941
21.58	$L^{13}R$	1	14	0.07142857143
21.57	$L^{12}R$	1	13	0.07692307692
21.56	$L^{11}R$	1	12	0.08333333333
21.53	$L^{9}R$	1	10	0.1
21.5	$L^{8}R$	1	9	0.1111111111
21.49	$L^{8}RL^{7}R$	2	17	0.1176470588
21.47	$L^{7}R$	1	8	0.125
21.43	$L^{6}R$	1	7	0.1428571429
21.42	$L^{6}R$	1	7	0.1428571429
21.4	$L^{6}RL^{5}R$	2	13	0.1538461538
21.39	$L^{6}RL^{5}RL^{5}R$	3	19	0.1578947368
21.38	$L^{6}RL^{5}RL^{5}RL^{5}RL^{5}RL^{5}RL^{5}RL^{5}R$	7	43	0.1627906977
21.37	$L^{5}R$	1	6	0.1666666667
$\vdots$	$\vdots$	$\vdots$	$\vdots$	$\vdots$
21.34	$L^{5}R$	1	6	0.1666666667

τ	Minimal Sequence	r	n	η number
21.31	L^5RL^4R	2	11	0.1818181818
21.3	$L^5RL^4RL^4R$	3	16	0.1875
21.29	$L^5RL^4RL^4RL^4RL^4R$	5	26	0.1923076923
21.28	L^4R	1	5	0.2
⋮	⋮	⋮	⋮	⋮
21.2	L^4R	1	5	0.2
21.19	$L^4RL^4RL^3R$	3	14	0.2142857143
21.17	L^4RL^3R	2	9	0.2222222222
21.16	L^4RL^3R	2	9	0.2222222222
21.15	$L^4RL^3RL^3R$	3	13	0.2307692308
21.14	$L^4RL^3RL^3RL^3R$	4	17	0.2352941176
21.13	$L^4RL^3RL^3RL^3RL^3RL^4RL^3RL^3RL^3RL^3RL^3RL^4$ $RL^3RL^3RL^3RL^3RL^3RL^4RL^3RL^3RL^3RL^3RL^3R$	23	96	0.2395833333
21.12	$L^4RL^3RL^3RL^3RL^3RL^3RL^3RL^3RL^3RL^3RL^3RL^3$ $RL^3RL^3RL^3RL^3RL^3RL^3RL^3RL^3RL^4RL^3RL^3RL^3$ $RL^3RL^3RL^3RL^3RL^3RL^3RL^3RL^3RL^3RL^3RL^3RL^3$ $RL^3RL^3RL^3RL^3RL^3R$	41	166	0.2469879518
21.11	L^3R	1	4	0.25
⋮	⋮	⋮	⋮	⋮
20.93	L^3R	1	4	0.25
20.92	L^7R	1	8	0.125
20.91	$L^3RL^3RL^2RL^3RL^2R$	5	18	0.2777777778
20.9	L^3RL^2R	2	7	0.2857142857
⋮	⋮	⋮	⋮	⋮
20.86	L^3RL^2R	2	7	0.2857142857
20.85	$L^3RL^2RL^2RL^3RL^2RL^2RL^3RL^2RL^3RL^2RL^2RL^3R$	17	57	0.298245614
20.84	$L^3RL^2RL^2R$	3	10	0.3
20.82	$L^3RL^2RL^2RL^2R$	4	13	0.3076923077
20.81	$L^3RL^2RL^2RL^2RL^2R$	5	16	0.3125
20.8	$L^3RL^2RL^2RL^2RL^2RL^2RL^2RL^2R$	8	25	0.32

τ	Minimal Sequence	r	n	η number
20.79	$L^3RL^2RL^2RL^2RL^2RL^2RL^2RL^2RL^2RL^2RL^2RL^2$ $RL^2RL^2RL^2RL^2RL^2RL^2RL^2RL^2RL^2RL^2RL^2$ $RL^2RL^2RL^2RL^2RL^2RL^2RL^2RL^2RL^2RL^2RL^2$ $RL^2RL^2RL^2RL^2RL^2R$	39	118	0.3305084746
20.78	L^2R	1	3	0.3333333333
⋮	⋮	⋮	⋮	⋮
20.15	L^2R	1	3	0.3333333333
20.14	L^2RL^2RLR	3	8	0.375
20.13	$L^2RL^2RLRL^2RLRL^2RLR$	7	18	0.3888888889
20.12	L^2RLR	2	5	0.4
⋮	⋮	⋮	⋮	⋮
20.01	L^2RLR	2	5	0.4
19.99	L^2RLRLR	3	7	0.4285714286
⋮	⋮	⋮	⋮	⋮
19.95	L^2RLRLR	3	7	0.4285714286
19.94	$L^2RLRLRLR$	4	9	0.4444444444
19.93	$L^2RLRLRLR$	4	9	0.4444444444
19.91	$L^2RLRLRLRLR$	5	11	0.4545454545
19.9	$L^2RLRLRLRLRLR$	6	13	0.4615384615
19.89	$L^2RLRLRLRLRLRLR$	7	15	0.4666666667
19.88	$L^2RLRLRLRLRLRLRLRLRLR$	10	21	0.4761904762
19.87	$L^2RLRLRLRLRLRLRLRLRLRLRLRLRLRLR$ $LRLRLR$	18	37	0.4864864865
19.86	LR	1	2	0.5
⋮	⋮	⋮	⋮	⋮
19.5	LR	1	2	0.5

Appendix B

Symbolic Sequences with Varying k

k	Minimal Sequence	r	n	η number
-0.877	$L^{102}R$	1	103	0.009708737864
-0.876	$L^{24}R$	1	25	0.04
-0.875	$L^{17}RL^{16}RL^{16}RL^{16}R$	4	69	0.05797101449
-0.874	$L^{13}R$	1	14	0.07142857143
-0.873	$L^{11}R$	1	12	0.08333333333
-0.872	$L^{10}RL^{10}RL^{9}R$	3	32	0.09375
-0.871	$L^{9}RL^{9}RL^{8}RL^{9}RL^{8}R$	5	48	0.1041666667
-0.87	$L^{8}R$	1	9	0.1111111111
-0.869	$L^{7}R$	1	8	0.125
-0.868	$L^{7}R$	1	8	0.125
-0.867	$L^{6}R$	1	7	0.1428571429
-0.866	$L^{6}R$	1	7	0.1428571429
-0.865	$L^{6}RL^{5}R$	2	13	0.1538461538
-0.864	$L^{5}R$	1	6	0.1666666667
-0.863	$L^{5}R$	1	6	0.1666666667
-0.862	$L^{5}R$	1	6	0.1666666667

k	Minimal Sequence	r	n	η number
-0.861	$L^5RL^5RL^4RL^5RL^4RL^5RL^4RL^5RL^4RL^5RL^4RL^5$ $RL^4RL^5RL^4RL^5RL^4RL^5RL^4RL^5RL^4R$ $L^5RL^4RL^5RL^4RL^5RL^4RL^5L^4RL^5RL^4RL^5RL^4$ $RL^5RL^4RL^5RL^4RL^5RL^4RL^5RL^4RL^5RL^4RL^5R$ $L^4RL^5RL^4R$	49	270	0.1814814815
-0.86	$L^5RL^4RL^4RL^4RL^4RL^4RL^4R$	7	36	0.1944444444
-0.859	L^4R	1	5	0.2
⋮	⋮	⋮	⋮	⋮
-0.855	L^4R	1	5	0.2
-0.854	$L^4RL^4RL^3R$	3	14	0.2142857143
-0.853	$L^4RL^3RL^3R$	3	13	0.2307692308
-0.852	L^3R	1	4	0.25
⋮	⋮	⋮	⋮	⋮
-0.84	L^3R	1	4	0.25
-0.839	L^3RL^2R	2	7	0.2857142857
-0.838	$L^3RL^2RL^2R$	3	10	0.3
-0.837	$L^3RL^2RL^2RL^2RL^2R$	5	16	0.3125
-0.836	L^2R	1	3	0.3333333333
⋮	⋮	⋮	⋮	⋮
-0.799	L^2R	1	3	0.3333333333
-0.798	L^2RLR	2	5	0.4
-0.797	L^2RLR	2	5	0.4
-0.796	L^2RLR	2	5	0.4
-0.795	L^2RLR	2	5	0.4
-0.794	L^2RLRLR	3	7	0.4285714286
-0.793	$L^2RLRLRLR$	4	9	0.4444444444
-0.792	$L^2RLRLRLRLRLRLRLRLRLRLR$	11	23	0.4782608696
-0.791	LR	1	2	0.5
⋮	⋮	⋮	⋮	⋮
-0.268	LR	1	2	0.5
-0.267	$LRLRLRLRLRLRLRLRLRLRLRLRLR^3$	15	28	0.5357142857
-0.266	$LRLRLRLRLRLR^3$	9	16	0.5625

k	Minimal Sequence	r	n	η number
-0.265	$LRLRLRLRLR^3$	7	12	0.5833333333
-0.264	$LRLRLRLR^3$	6	10	0.6
-0.263	$LRLRLRLR^3LRLRLR^2$	10	17	0.5882352941
-0.261	$LRLRLR^3LRLR^2$	8	13	0.6153846154
-0.26	$LRLRLR^2$	4	7	0.5714285714
-0.259	$LRLR^3$	4	6	0.6666666667
-0.257	$LRLR^2$	3	5	0.6
⋮	⋮	⋮	⋮	⋮
-0.252	$LRLR^2$	3	5	0.6
-0.251	$LRLR^3LR^3LR^3LR^2$	12	17	0.7058823529
-0.249	LR^2	2	3	0.6666666667
⋮	⋮	⋮	⋮	⋮
-0.209	LR^2	2	3	0.6666666667

Bibliography

[1] K. T. Alligood, T. D. Sauer, and J. A. Yorke, *Chaos: an Introduction to Dynamical Systems*, Springer, 1997.

[2] I. Ameen, S. Rida, A. El-Sayed, and A. Abdel-Rady, *On some impulsive differential equations*, Mathematical Sciences Letters, (2012), pp. 105–113.

[3] M. Bernardo, C. Budd, A. R. Champneys, and P. Kowalczyk, *Piecewise-smooth dynamical systems: theory and applications*, vol. 163, Springer Science & Business Media, 2008.

[4] P. Blanchard, R. L. Devaney, and G. R. Hall, *Differential Equations*, Cengage Learning, 2011.

[5] A. Dhooge, W. Govaerts, and Y. A. Kuznetsov, *Matcont: a matlab package for numerical bifurcation analysis of odes*, ACM Transactions on Mathematical Software (TOMS), 29 (2003), pp. 141–164.

[6] A. Dhooge, W. Govaerts, Y. A. Kuznetsov, H. G. E. Meijer, and B. Sautois, *New features of the software matcont for bifurcation analysis of dynamical systems*, Mathematical and Computer Modelling of Dynamical Systems, 14 (2008), pp. 147–175.

[7] A. Granados, L. Alsedà, and M. Krupa, *The period adding and incrementing bifurcations: From rotation theory to applications*, SIAM Review, 59 (2017), pp. 225–292.

[8] M. W. Hirsch, S. Smale, and R. L. Devaney, *Differential equations, dynamical systems, and an introduction to chaos*, Elsevier Academic Press, 2013.

[9] A. Hoyer-Leitzel and S. Iams, *Impulsive fire disturbance in a savanna model: Tree–grass coexistence states, multiple stable system states, and resilience*, Bulletin of Mathematical Biology, 83 (2021), p. 113.

[10] C. Liu, S. Su, and B. Zhu, *A flow-kick fitzhugh-nagumo model with stochastic perturbation*, 2023. Poster Presentation.

[11] K. Meyer, A. Hoyer-Leitzel, S. Iams, I. Klasky, V. Lee, S. Ligtenberg, E. Bussmann, and M. L. Zeeman, *Quantifying resilience to recurrent ecosystem disturbances using flow–kick dynamics*, Nature Sustainability, 1 (2018), pp. 671–678.

[12] K. J. Meyer, H. Fusco, C. Smith, and A. Hoyer-Leitzel, *Continuation of fixed points and bifurcations from ode to flow-kick disturbance models*, SIAM Journal on Applied Dynamical Systems, 23 (2024), pp. 2983–3012.

[13] S. H. Strogatz, *Nonlinear dynamics and chaos: with applications to physics, biology, chemistry, and engineering*, Chapman and Hall/CRC, 2024.

[14] S. Wiggins, *Introduction to applied nonlinear dynamical systems and chaos*, Springer, 2003.

[15] M. L. Zeeman, K. Meyer, E. Bussmann, A. Hoyer-Leitzel, S. Iams, I. J. Klasky, V. Lee, and S. Ligtenberg, *Resilience of socially valued properties of natural systems to repeated disturbance: A framework to support value-laden management decisions*, Natural Resource Modeling, 31 (2018), p. e12170.